Performance-Based Bi-Objective Optimization of Structural Systems Subject to Stochastic Wind Excitation

Arthriya Subgranon[b], Seymour M.J. Spence[a,1,*]

[a]*Department of Civil and Environmental Engineering, University of Michigan, Ann Arbor, MI 48109, USA*
[b]*Department of Civil and Coastal Engineering, University of Florida, Gainesville, FL 32611, USA*

Abstract

This paper outlines the development of a stochastic simulation-based design optimization approach for dynamic wind excited structures in which correlations between component damages and losses are explicitly treated. The proposed approach integrates a bi-objective design optimization scheme with a probabilistic performance-based wind engineering methodology which systematically accounts for the various sources of uncertainties involved in system loss estimation. Through the ϵ-constraint technique, the bi-objective optimization problem is transformed into a series of single-objective stochastic optimization problems. To solve each ϵ-constraint optimization problem, a pseudo-simulation scheme is proposed that allows for the formulation of an approximate sub-problem that can be solved sequentially to identify solutions that define a set of Pareto optimal designs. In the proposed scheme, samples of engineering demands are approximated in terms of auxiliary variable vectors, which are by-products of an augmented simulation carried out in a fixed design point. Analytical expressions are derived that relate the engineering demand samples to the second-order statistics of wind-induced losses based on the concept of fragility. Potential correlations between the component capacities and component losses are explicitly treated. The effectiveness of the proposed approach and its scalability to high-dimensional problems are illustrated through optimal designs of moment-resisting frames subject to stochastic wind loads.

Keywords: Bi-objective optimization, Performance-based design, Wind engineering, System-level loss assessment, Stochastic wind loads, High-dimensional problems

---

*Corresponding author
Email addresses: arthriya@ufl.edu (Arthriya Subgranon), smjs@umich.edu (Seymour M.J. Spence)
[1]Tel. +1-734-764-8419, Fax +1-734-764-4292

1. Introduction

In developing risk management strategies, the integration of bi-objective design optimization (BODO) schemes with performance assessment frameworks, provides an attractive decision support space in which useful insights into the trade-offs between upfront cost and anticipated losses can be obtained [1–7]. For wind excited buidlings, stochastic performance-based wind engineering (PBWE) frameworks can be used to directly assess performance metrics that systematically treat various sources of uncertainties [8–15]. However, the computational effort in repeatedly performing the stochastic simulation for different designs during the optimization process is complex and time-consuming, especially for large-scale systems that involve high-fidelity models and a large number of design variables. To overcome these challenges, the authors have recently proposed an efficient method that is based on transforming the performance-based BODO problem into a series of single-objective stochastic optimization problems through the ϵ-constraint technique [6]. By solving a series of problems for various values of ϵ, a set of the searched-after Pareto optimal solutions can be identified. To solve each ϵ-constraint problem, Suksuwan and Spence [6] proposed a method based on formulating and solving a sequence of sub-problems: this method allows a probabilistic loss measure to be updated during the optimization through kriging metamodels that are constructed from results of a stochastic simulation. While the kriging-based approach is computationally efficient for large-scale problems, the method does not consider correlations between damage states or correlations between component losses. These correlations, however, can significantly affect the total loss [e.g. 16, 17], and should therefore be treated during not only the loss assessment, but also the optimization process.

In general, there are three types of correlations that may have a significant impact on the total loss of a system: (i) correlation between engineering demand parameters (EDP), given that a windstorm of prescribed intensity has occurred; (ii) correlation between component damage states (DS), given engineering demands; and (iii) correlation between component decision variables/losses (DVC), given damage states. While the correlation in the conditional demand level can be estimated directly from the results of structural response analysis, the same cannot be said for conditional correlations at the damage state and the component loss levels. To date, few models have been proposed for treating such inter-component correlations. In the field of earthquake engineering, Baker and Cornell [16] proposed a seismic loss estimation approach that considers inter-component correlations through a first-order second-moment (FOSM) analysis method in which the mean and variance of the total loss is estimated conditional on earthquake intensity. Through this approach, the conditional damage state given an engineering demand ($DS|EDP$) and conditional component loss given a damage state ($DVC|DS$) were collapsed into a $DVC|EDP$ relationship, while a generalized equi-correlated model is proposed to estimate the correlation in the collapsed relationship. Aslani [18] proposed an approach that utilizes the FOSM method in computing the covariance terms when estimating the standard deviation of the total loss, while the correlation of $DS|EDP$ is estimated through an iterative procedure with the correlation of $DVC|DS$ obtained from data pertaining to construction cost. In seismic design practice, the Federal Emergency Management Agency (FEMA) P-58 guidelines [19] assume damage states in the same performance group to either be perfectly correlated or uncorrelated, while the case of partially correlated components is omitted. To incorporate partial correlations, while avoiding potential errors incurred in using the FOSM approximation, Bradley and Lee [17] proposed a tractable analytical approach to seismic loss assessment that can explicitly consider the correlations in the conditional demands, conditional damage states, and conditional component losses.

This work aims to develop a new approach for solving the ϵ-constraint problem oulined in [20] that is capable of treating general inter-component correlations. In particular, as loss measures, both the expected value and variance are considered, while correlations in the damage capacity and component losses are explicitly modeled based on the approaches outlined in [17]. The basic idea of the proposed method is to derive closed-form relationships between samples of engineering demands and the second-order statistics of wind-induced losses based on the knowledge of the fragility and consequence functions. By substituting in the derived expressions with demand samples approximated in terms of auxiliary variable vectors [20, 21], a pseudo-simulation scheme is defined that can be used to formulate an approximate sub-problem that enables the use of gradient-based optimization algorithms. Within this setting, the probabilistic loss measure, as well as inter-component correlations, can be efficiently updated during the optimization process without the need to invoke any dynamic structural analysis or calibrate any metamodels. The validity of the proposed approach is illustrated first through the optimal design of a lateral load-resisting system of a two-story building. The practicality of the approach is then demonstrated through the identification of set of Pareto optimal designs of a multistory building system subject to stochastic wind loads.

2. Problem Statement

To provide decision-makers with trade-off information regarding various design options, it is of interest to identify a set of optimal designs that simultaneously minimize the initial cost of the system as well as the anticipated losses caused by extreme windstorms. This engineering problem can be formulated in terms of the following bi-objective optimization problem:

$$\begin{aligned} &\text{Find} \qquad \mathbf{x} = \{x_1, ..., x_N\}^T \\ &\text{to minimize} \qquad [V(\mathbf{x}), L(\mathbf{x}; im)] \\ &\text{subject to} \quad x_n \in \mathbb{X}_n \quad n = 1, \dots, N \end{aligned} \tag{1}$$

where $\mathbf{x}$ is a high-dimensional design variable vector collecting the N deterministic parameters that are used to define the structural system (e.g. structural member sizes); V is a function associated with the initial cost of the structural system (e.g. volume of structural material) and is assumed to be deterministic and explicit in $\mathbf{x}$; L is a probabilistic function describing a system-level loss measure for a wind event of prescribed intensity measure $IM = im$ (e.g. a site specific wind speed with a mean recurrence interval (MRI) of 700 years); while $\mathbb{X}_n$ is the set of discrete values to which the nth component of $\mathbf{x}$ must belong. In particular, L is defined here as:

$$L(\mathbf{x}; im) = \mu_{DV|IM}(\mathbf{x}; im) + \alpha \cdot \sigma_{DV|IM}(\mathbf{x}; im) \tag{2}$$

where $\mu_{DV|IM}$ and $\sigma_{DV|IM}$ are the expected value and standard deviation, respectively, of the system-level decision variable DV (e.g. total repair cost) conditioned on IM; while α is a parameter, $\alpha \geq 0$, whose value can be assigned according to the desired level of design robustness. In other words, a larger α assigns more weight to the standard deviation in order to restrict the variability in the system-level loss, hence increasing the design robustness [6].

3. Loss Assessment Framework Considering Component Correlations

3.1. Overview of the Methodology

This section introduces an efficient framework for estimating the loss measure, L, for a given design $\mathbf{x}$ and wind event of intensity im, while explicitly accounting for component correlations. In general, the components of a system that are susceptible to damage due to a common demand parameter can be grouped to define what is known as a performance group (PG) [19]. The total loss, DV, can then be seen as the sum of losses over all PGs defining the system, and therefore as:

$$DV(\mathbf{x}; im) = \sum_{j=1}^{N_G} DV_j(\mathbf{x}; im) \tag{3}$$

where N_G is the total number of PGs defining the system, while DV_j is a group-level decision variable associated with the jth PG (e.g. repair cost associated with cladding components on the first floor). Based on Eq. (3), the second-order statistics of DV can be estimated in terms of the group-level losses as follows:

$$\mu_{DV|IM}(\mathbf{x}; im) = \sum_{j=1}^{N_G} \mu_{DV_j|IM}(\mathbf{x}; im) \tag{4}$$

$$\sigma_{DV|IM}(\mathbf{x}; im) = \sqrt{\sum_{j=1}^{N_G} \sum_{k=1}^{N_G} \sigma_{DV_j,DV_k|IM}(\mathbf{x}; im)} \tag{5}$$

where $\mu_{DV|IM}$ and $\sigma_{DV|IM}$ are the conditional expected value and standard deviation of DV; $\mu_{DV_j|IM}$ is the conditional expected value of DV_j; while $\sigma_{DV_j,DV_k|IM}$ is the conditional covariance between DV_j and DV_k given that $IM = im$.

The loss associated with each PG depends on the current damage states of each component of the PG, and therefore the response level of the associated engineering demand parameter (e.g. inter-story drift). In this respect, the following functional relationships can be derived between the demand and the group-level loss statistics (where the dependence on $\mathbf{x}$ and IM is dropped for clarity):

$$\mu_{DV_j} = \mathrm{E}[\mu_{DV_j|EDP_j}] \tag{6}$$

$$\sigma_{DV_j,DV_k} = \mathrm{E}[\sigma_{DV_j,DV_k|EDP_j,EDP_k}] + \mathrm{Cov}[\mu_{DV_j|EDP_j}, \mu_{DV_k|EDP_k}] \tag{7}$$

where $\mu_{DV_j|EDP_j}$ is the mean of DV_j conditioned on the engineering demand parameter, EDP_j; $\mu_{DV_k|EDP_k}$ is the mean of DV_k conditioned on EDP_k; $\sigma_{DV_j,DV_k|EDP_j,EDP_k}$ is the covariance between DV_j and DV_k conditioned on EDP_j and EDP_k; while E[·] and Cov[·] denote the expectation and covariance operators, respectively.

For a given design $\mathbf{x}$, the second-order statistics are affected by many uncertainties, including the aleatory nature of the wind, uncertainties in the system parameters, uncertainties in the damage and consequence assessment, and epistemic uncertainties in the mathematical modeling. Hence, the loss assessment generally involves a large number of random variables with different corresponding distributions. To systematically carry out probabilistic analysis within this high-dimensional uncertain space, a Monte Carlo simulation technique is adopted in this work. Through the Monte Carlo method, the expected value of a random variable Y_j (e.g. $\mu_{DV_j|EDP_j}$ and $\sigma_{DV_j,DV_k|EDP_j,EDP_k}$ introduced in this section) may be estimated as:

$$\mathrm{E}[Y_j] \approx \frac{1}{N_s}\sum_{i=1}^{N_s} y_j(edp_j^{(i)}) \tag{8}$$

where N_s is the total number of samples used in the simulation, while $edp_j^{(i)}$ is the ith realization of EDP_j. Similarly, the covariance between any two variables Y_j and Y_k can also be estimated from the samples as:

$$\mathrm{Cov}[Y_j, Y_k] \approx \frac{1}{N_s - 1}\sum_{i=1}^{N_s}\left[y_j(edp_j^{(i)}) - \mathrm{E}[Y_j]\right]\cdot\left[y_k(edp_k^{(i)}) - \mathrm{E}[Y_k]\right] \tag{9}$$

To this end, an efficient method to generate realizations of a vector of correlated engineering demand parameters, $\mathbf{EDP} = \{EDP_1, ..., EDP_{N_g}\}^T$, and a method that can quickly evaluate the conditional statistics given **EDP** are needed. Throughout this paper, uppercase letters (e.g. Y_j) are used to represent random variables, while lowercase letters (e.g. y_j) are used to represent realizations.

3.2. Engineering Demand Parameters

This section provides a brief overview of the approach used in this work to generate samples of the EDPs. Detailed derivations of the equations and descriptions of the models can be found in [6, 20, 22] and are provided for convenience in Appendix A, regarding the estimation of resonant modal response, and in Appendix B regarding the estimation of stochastic wind loads.

For the following damage analysis, the EDPs are defined as the absolute peak responses of a structural system subject to a wind event of duration T. Hence, a realization of an element of **EDP** can be written as:

$$edp_j^{(i)}(\mathbf{u}^{(i)}) = \max_{\beta \in [0,2\pi]} \left\{ \max_{t \in [0,T]} |r_j^{(i)}(t;\beta,\mathbf{u}^{(i)})| \right\} \tag{10}$$

where i denotes the realization, $\mathbf{u}^{(i)}$ is the ith sample of a high-dimensional uncertain vector $\mathbf{U}$ that contains all uncertain variables considered in the estimation of the EDPs (examples of these variables and possible distributions are provided in Table B.4), β denotes the wind direction, and $r_j^{(i)}(t)$ represents the ith realization of the response process time-history associated with the jth PG. In particular, the stochastic response process can be efficiently estimated through the following load-effect model [21]:

$$r_j^{(i)}(t;\beta,\mathbf{u}^{(i)}) = s_1^{(i)} \left[\mathbf{\Gamma}_j^T \mathbf{f}(t;\beta,\bar{v}_H,\mathbf{u}^{(i)}) + \mathbf{\Gamma}_j^T \mathbf{K} \mathbf{\Phi}_M \mathbf{q}_{R_M}(t;\beta,\bar{v}_H,\mathbf{u}^{(i)}) \right] \tag{11}$$

where S_1 represents a random variable modeling the epistemic uncertainty in the load-effect model and is an element of $\mathbf{U}$; $\mathbf{\Gamma}_j$ is a vector containing influence functions, each giving the response in r_j due to a unit load acting at a given degree of freedom of the system; $\mathbf{f}(t)$ is a vector-valued stochastic wind process calibrated to a site-specific wind speed $\bar{v}_H$ that is averaged over a time duration T; $\mathbf{K}$ is the stiffness matrix of the system; $\mathbf{\Phi}_M$ is the mass normalized mode shape matrix considering the first M modes; and $\mathbf{q}_{R_M}(t)$ is a vector whose elements are resonant modal displacement response processes associated with the first M modes. A procedure to estimate $\mathbf{q}_{R_M}(t)$ is provided in Appendix A.

To rapidly generate realizations of the stochastic wind loads, $\mathbf{f}(t)$, to be used in the response model of Eq. (11), this work adopts a proper orthogonal decomposition (POD)-based method [23]. The POD-based stochastic wind model is described in more details in Appendix B. It should be noted that the proposed framework is not restricted to any particular stochastic wind model. The choice of the POD-based model is due to its efficiency while enabling the use of wind tunnel data, which can account for complex aerodynamic phenomena such as vortex shedding.

3.3. Estimation of the Conditional Statistics

3.3.1. Conditional Expectation

Once a sample of the engineering demand is obtained through Eq. (10), a realization of the conditional expected value of a group-level loss, $\mu_{DV_j|EDP_j}$, may be estimated through a summation over the components in the group as:

$$\mu_{DV_j|EDP_j}(edp_j^{(i)}) = \sum_{m=1}^{N_{C_j}} \mu_{DVC_{jm}|EDP_j}(edp_j^{(i)}) \tag{12}$$

where i represents the sample number, N_{C_j} is the total number of components in the jth PG, and $\mu_{DVC_{jm}|EDP_j}$ is the conditional expected loss associated with component m. For a component m that is susceptible to N_{DS_m} possible damage states, $\mu_{DVC_{jm}|EDP_j}$ may be directly estimates from the fragility functions as:

$$\mu_{DVC_{jm}|EDP_j}(edp_j^{(i)}) = \sum_{q=0}^{N_{DS_m}} \mu_{DVC_{jm}|DS_m}(q) \cdot \left[\mathrm{Fr}_q(edp_j^{(i)}) - \mathrm{Fr}_{q+1}(edp_j^{(i)})\right] \tag{13}$$

where $\mu_{DVC_{jm}|DS_m}(q)$ denotes the expected component loss given that the damage state q has occurred, while Fr_q and Fr_{q+1} are fragility functions associated with the damage states q and $q+1$, respectively, where $q = 0, ..., N_{DS_m}$ and $\mathrm{Fr}_{N_{DS_m}+1} = 0$ [20, 24].

3.3.2. Conditional Covariance

The conditional covariance between group-level losses can be formulated in terms of the conditional component correlations as:

$$\begin{aligned}\sigma_{DV_j,DV_k|EDP_j,EDP_k}(edp_j^{(i)}, edp_k^{(i)}) = \sum_{m=1}^{N_{C_j}} \sum_{n=1}^{N_{C_k}} \Big[&\rho_{DVC_{jm},DVC_{kn}|EDP_j,EDP_k}(edp_j^{(i)}, edp_k^{(i)}) \\ &\cdot \sigma_{DVC_{jm}|EDP_j}(edp_j^{(i)}) \cdot \sigma_{DVC_{kn}|EDP_k}(edp_k^{(i)})\Big]\end{aligned} \tag{14}$$

where N_{C_k} is the total number of components in the kth PG; $\rho_{DVC_{jm},DVC_{kn}|EDP_j,EDP_k}$ is the conditional correlation coefficient between the loss associated with component m in the jth PG, DVC_{jm}, and the loss associated with component n in the kth PG, DVC_{kn}; while $\sigma_{DVC_{jm}|EDP_j}$ and $\sigma_{DVC_{kn}|EDP_k}$ are the standard deviation of DVC_{jm} and DVC_{kn}, conditioned on EDP_j and EDP_k, respectively. Analogous to the conditional mean, for a component m

that is susceptible to N_{DS}^m damage states, $\sigma_{DVC_{jm}|EDP_j}$ may be calculated as [24]:

$$\sigma_{DVC_{jm}|EDP_j}(edp_j^{(i)}) = \Bigg[\sum_{q=0}^{N_{DS}^m} \sigma^2_{DVC_{jm}|DS_m}(q) \cdot \Big(\mathrm{Fr}_q(edp_j^{(i)}) - \mathrm{Fr}_{q+1}(edp_j^{(i)})\Big) + \sum_{q=0}^{N_{DS}^m} (\mu_{DVC_{jm}|DS_m}(q) - \mu_{DVC_{jm}|EDP_j}(edp_j^{(i)}))^2 \cdot \Big(\mathrm{Fr}_q(edp_j^{(i)}) - \mathrm{Fr}_{q+1}(edp_j^{(i)})\Big) \Bigg]^{\frac{1}{2}} \tag{15}$$

where $\sigma^2_{DVC_{jm}|DS_m}(q)$ is the variance of DVC_{jm} given that damage state q has occurred.

The conditional correlations posed in Eq. (14) may be expressed as:

$$\rho_{DVC_{jm},DVC_{kn}|EDP_j,EDP_k}(edp_j^{(i)}, edp_k^{(i)}) = \frac{\mu_{DVC_{jm}DVC_{kn}|EDP_j,EDP_k}(edp_j^{(i)}, edp_k^{(i)}) - \mu_{DVC_{jm}|EDP_j}(edp_j^{(i)}) \cdot \mu_{DVC_{kn}|EDP_k}(edp_k^{(i)})}{\sigma_{DVC_{jm}|EDP_j}(edp_j^{(i)}) \cdot \sigma_{DVC_{kn}|EDP_k}(edp_k^{(i)})} \tag{16}$$

where $\mu_{DVC_{jm}DVC_{kn}|EDP_j,EDP_k}$ is the conditional expected value of the product of DVC_{jm} and DVC_{kn} that can be formulated in terms of component damage states based on the total probability theorem as (for detailed derivations see Appendix C):

$$\mu_{DVC_{jm}DVC_{kn}|EDP_j,EDP_k}(edp_j^{(i)}, edp_k^{(i)}) = \sum_{q=1}^{N_{DS}^m} \sum_{r=1}^{N_{DS}^n} \Big[\Big(\rho_{DVC_{jm},DVC_{kn}|DS_m,DS_n}(q,r) \cdot \sigma_{DVC_{jm}|DS_m}(q) \cdot \sigma_{DVC_{kn}|DS_n}(r) + \mu_{DVC_{jm}|DS_m}(q) \cdot \mu_{DVC_{kn}|DS_n}(r)\Big) \cdot \mathrm{P}_{DS_m,DS_n|EDP_j,EDP_k}(q, r|edp_j^{(i)}, edp_k^{(i)})\Big] \tag{17}$$

where $\rho_{DVC_{jm},DVC_{kn}|DS_m,DS_n}(q,r)$ is the correlation between the mth and the nth component losses due to damage states q and r; $\sigma_{DVC_{jm}|DS_m}(q)$ and $\sigma_{DVC_{kn}|DS_n}(r)$ are the standard deviations of DVC_{jm} and DVC_{kn} conditioned on the damage state q and r; while $\mathrm{P}_{DS_m,DS_n|EDP_j,EDP_k}$ is the conditional joint probability of the mth and the nth component damage state given EDP_j and EDP_k. In particular, $\mathrm{P}_{DS_m,DS_n|EDP_j,EDP_k}$ can be determined from appropriate fragility functions as [17]:

$$\mathrm{P}_{DS_m,DS_n|EDP_j,EDP_k}(q, r|edp_j^{(i)}, edp_k^{(i)}) = \mathrm{Fr}_{DS_m,DS_n|EDP_j,EDP_k}(q, r|edp_j^{(i)}, edp_k^{(i)}) - \sum_{v=q}^{N_{DS}^m} \sum_{\substack{w=r \\ q \neq r \text{ if } v=q}}^{N_{DS}^n} \mathrm{P}_{DS_m,DS_n|EDP_j,EDP_k}(v, w|edp_j^{(i)}, edp_k^{(i)}) \tag{18}$$

where $\mathrm{Fr}_{DS_m,DS_n|EDP_j,EDP_k}(q,r|edp_j^{(i)},edp_k^{(i)}) = \mathrm{P}(DS_m \geq q, DS_n \geq r|edp_j^{(i)},edp_k^{(i)})$ denotes a joint fragility function defined as the conditional joint probability that component m will have the damage state q or worse, while component n will have the damage state r or worse given $EDP_j = edp_j^{(i)}$ and $EDP_k = edp_k^{(i)}$. Analogous to a typical fragility function that is assumed to follow a lognormal distribution, the joint fragility is assumed here to have a bi-variate lognormal distribution. It is of interest to write the joint fragility function in terms of a component damage capacity (i.e. the demand level at which the component enters a specified damage state), and therefore in the following form:

$$\begin{aligned}
&\mathrm{Fr}_{DS_m,DS_n|EDP_j,EDP_k}(q,r|edp_j^{(i)},edp_k^{(i)}) \\
&\quad = \mathrm{P}(\ln C_{m,q} < \ln edp_j^{(i)}, \ln C_{n,r} < \ln edp_k^{(i)}) \\
&\quad = \iint\limits_{\substack{\ln c_{m,q} < \ln edp_j^{(i)} \\ \ln c_{n,r} < \ln edp_k^{(i)}}} \frac{1}{\sqrt{|\mathbf{C}_{\ln C}|(2\pi)^2}} \exp\left(-\frac{1}{2}(\mathbf{z}_{\ln edp} - \boldsymbol{\mu}_{\ln C})\mathbf{C}^{-1}_{\ln C_m, \ln C_n}(\mathbf{z}_{\ln edp} - \boldsymbol{\mu}_{\ln C})^T\right) \mathrm{d}\ln c_{m,q} \mathrm{d}\ln c_{n,r}
\end{aligned} \tag{19}$$

where $C_{m,q}$ and $C_{n,r}$ are the capacities associated with the damage states q and r of the components m and n, respectively; $\mathbf{C}_{\ln C}$ is the covariance matrix of the component capacities that can be defined as:

$$\mathbf{C}_{\ln C} = \begin{bmatrix} \sigma^2_{\ln c_{m,q}} & \rho_{\ln c_{m,q}, \ln c_{n,r}} \sigma_{\ln c_{m,q}} \sigma_{\ln c_{n,r}} \\ \rho_{\ln c_{n,r}, \ln c_{m,q}} \sigma_{\ln c_{n,r}} \sigma_{\ln c_{m,q}} & \sigma^2_{\ln c_{n,r}} \end{bmatrix} \tag{20}$$

where $\rho_{\ln c_{n,r}, \ln c_{m,q}}$ denotes the correlation coefficient between the component capacities; $\mathbf{z}_{\ln edp} = \{\ln edp_j^{(i)}, \ln edp_k^{(i)}\}^T$ is a vector collecting the natural log of the demands; while $\boldsymbol{\mu}_{\ln C} = \{\mu_{\ln C_{m,q}}, \mu_{\ln C_{n,r}}\}^T$ is a vector collecting the means of the component capacities. The advantages of Eq. (19) are threefold: 1) it allows for the direct implementation of any efficient numerical algorithm for solving for the cumulative bi-variate normal distribution; 2) the correlation coefficient between the damage state capacities ,$\rho_{\ln C_{m,q}, \ln C_{n,r}}$, can be modeled independent of the engineering demand parameters and therefore independent of the design variables; and 3) it allows for derivation of a closed-form gradient function that helps accelerate the optimization process (see details in Sec. 4.2.1).

4. Proposed Optimization Strategy

To efficiently solve the bi-objective stochastic optimization problem of the type posed in Eq. (1), the authors have demonstrated in [6] that the ϵ-constraint approach can be used to transform the original problem into a series of single-objective optimization problems. By turning the loss measure into a constraint, the ϵ-constraint problem is formulated as:

$$\begin{aligned} &\text{Find} \quad \mathbf{x} = \{x_1, ..., x_N\}^T \\ &\text{to minimize} \quad V(\mathbf{x}) \\ &\text{subject to} \quad L(\mathbf{x}; im) = \mu_{DV|IM}(\mathbf{x}; im) + \alpha \cdot \sigma_{DV|IM}(\mathbf{x}; im) \leq \epsilon \\ &x_n \in \mathbb{X}_n \quad n = 1, \ldots, N \end{aligned} \tag{21}$$

where ϵ represents the threshold value that L must meet. By solving a series of these problems for various values of ϵ, a set of Pareto optimal solutions is identified. In other words, these optimal designs are such that one objective function cannot be further improved without depreciating the other objective function.

Although the original problem has been decomposed, solving a single-objective optimization problem of the type posed in Eq. (21) is still computationally cumbersome as it involves not only a time-consuming stochastic simulation, but also a large number of design variables if practical problems are considered. To handle this high-dimensional stochastic optimization problem, this work proposes a method that is based on constructing an approximation for the loss measure that is efficient to evaluate and can take into account changes in component correlations during the optimization.

4.1. Loss Measure Approximation

To estimate the loss measure, L, as defined in Eq. (2), it can be observed that the majority of the computational expense in estimating $\mu_{DV|IM}$ and $\sigma_{DV|IM}$ through the Monte Carlo simulation is allocated to the estimation of the EDP_j samples. This is because such an estimation involves performing a structural dynamic analysis of a large-scale finite element model subject to long duration stochastic wind loads. To circumvent this hurdle during the optimization process, this paper proposes a method that approximately decouples the structural dynamic analysis from the optimization process. The proposed method approximates samples of engineering demands in terms of auxiliary variable vectors, while utilizing the conditional statistics estimation scheme described in Sec. 3.3 to quickly update changes in the loss statistics.

4.1.1. Augmented Simulation Process

To construct an efficient approximation scheme that is insensitive to the number of design variables, the method centers on the definition of a reduce variate and an auxiliary variable vector [21, 22, 25] that can be fully defined from results of a single Monte Carlo simulation carried out in a fixed design point. Within this context, considering a simulation performed in the current design $\mathbf{x}_{mc}$, it is proposed that each sample of EDP_j can be written as:

$$edp_j^{(i)}(\mathbf{x}_{mc}) = \mu_{EDP_j}(\mathbf{x}_{mc}) + g_j^{(i)}(\mathbf{x}_{mc}) \cdot \sigma_{EDP_j}(\mathbf{x}_{mc}) \tag{22}$$

where μ_{EDP_j} and σ_{EDP_j} are the mean and standard deviation of EDP_j, respectively; and $g_j^{(i)}$ is a reduced variate associated with $edp_j^{(i)}$ and defined as:

$$g_j^{(i)}(\mathbf{x}_{mc}) = \frac{edp_j^{(i)}(\mathbf{x}_{mc}) - \mu_{EDP_j}(\mathbf{x}_{mc})}{\sigma_{EDP_j}(\mathbf{x}_{mc})} \tag{23}$$

Thus, for every demand sample, $edp_j^{(i)}$, there will be an associated $g_j^{(i)}$ that can be estimated once μ_{EDP_j} and σ_{EDP_j} are calculated at the end of the simulation process.

To define the auxiliary variable vector (AVV), used later in the demand approximation scheme to predict μ_{EDP_j} and σ_{EDP_j}, it is first necessary to define the following vector-valued stochastic variable for each realization:

$$\mathbf{F}^{(i)}(\mathbf{x}_{mc}; t, \mathbf{u}^{(i)}) = s_1^{(i)} \left[\mathbf{f}(t; \mathbf{u}^{(i)}) + \mathbf{K}(\mathbf{x}_{mc})\mathbf{\Phi}_M(\mathbf{x}_{mc})\mathbf{q}_{R_M}(\mathbf{x}_{mc}; t, \mathbf{u}^{(i)})\right] \tag{24}$$

Based on $\mathbf{F}^{(i)}(t)$, $r_j^{(i)}(t)$ and $edp^{(i)}$, the following stochastic variable associated with the ith realization may be defined:

$$\psi_j^{(i)}(\mathbf{x}_{mc}; \mathbf{u}^{(i)}) = \mu_{\mathbf{F}}(\mathbf{x}_{mc}; \mathbf{u}^{(i)}) + \frac{edp_j^{(i)}(\mathbf{x}_{mc}; \mathbf{u}^{(i)}) - \mu_{r_j}(\mathbf{x}_{mc}; \mathbf{u}^{(i)})}{\sigma_{r_j}^2(\mathbf{x}_{mc}; \mathbf{u}^{(i)})} \mathbf{C}_{\mathbf{F}}(\mathbf{x}_{mc}; \mathbf{u}^{(i)})\Gamma_j(\mathbf{x}_{mc}) \tag{25}$$

where $\mu_{\mathbf{F}}$ and $\mathbf{C}_{\mathbf{F}}$ are the mean and covariance matrix of $\mathbf{F}^{(i)}(t)$; while μ_{r_j} and σ_{r_j} are the mean and standard deviation of the response process, $r_j(t)$, respectively. From all realizations of $\psi_j^{(i)}$, the following AVVs can be defined:

$$\bar{\mathbf{\Psi}}_j(\mathbf{x}_{mc}) = \mu_{\psi_j}(\mathbf{x}_{mc}) \tag{26}$$

$$\hat{\mathbf{\Psi}}_j(\mathbf{x}_{mc}) = \frac{\mathbf{C}_{\mathbf{\Psi}}(\mathbf{x}_{mc})\Gamma_j(\mathbf{x}_{mc})}{\sigma_{EDP_j}(\mathbf{x}_{mc})} \tag{27}$$

where μ_{ψ_j} is the mean of ψ_j while $\mathbf{C}_{\mathbf{\Psi}}$ is the covariance matrix of $\mathbf{\Psi} = [\psi_1 ... \psi_j ... \psi_{N_j}]$. The AVVs, $\bar{\mathbf{\Psi}}_j$ and $\hat{\mathbf{\Psi}}_j$, are particularly useful as, when they are statically applied to the system, the resulting responses coincide with the second-order statistics of the engineering demands, i.e. the follow holds:

$$\mu_{EDP_j}(\mathbf{x}_{mc}) = \mathbf{\Gamma}_j^T(\mathbf{x}_{mc})\bar{\mathbf{\Psi}}_j(\mathbf{x}_{mc}) \tag{28}$$

$$\sigma_{EDP_j}(\mathbf{x}_{mc}) = \mathbf{\Gamma}_j^T(\mathbf{x}_{mc})\hat{\mathbf{\Psi}}_j(\mathbf{x}_{mc}) \tag{29}$$

These relationships are exact in $\mathbf{x}_{mc}$, i.e. where the Monte Carlo simulation was carried out.

4.1.2. Pseudo-Simulation Scheme

The reduced variates, $g_j^{(i)}$, and the AVVs, $\bar{\Psi}_j$ and $\hat{\Psi}_j$, can be seen as by-products of a single augmented simulation carried out in $\mathbf{x}_{mc}$. If it is assumed that $g_j^{(i)}$, $\bar{\Psi}_j$ and $\hat{\Psi}_j$ are insensitive to relatively small changes in $\mathbf{x}$ around $\mathbf{x}_{mc}$ during the optimization process, the demand samples may be approximated without invoking any dynamic structural analysis as:

$$\widetilde{edp}_j^{(i)}(\mathbf{x}) = \mathbf{\Gamma}_j^T(\mathbf{x})\bar{\mathbf{\Psi}}_j(\mathbf{x}_{mc}) + g_j^{(i)}(\mathbf{x}_{mc}) \cdot \mathbf{\Gamma}_j^T(\mathbf{x})\hat{\mathbf{\Psi}}_j(\mathbf{x}_{mc}) \tag{30}$$

The approximate demand sample of Eq. (30) allows for the following pseudo-simulation scheme to estimate the system-level loss statistics (i.e. Eqs. (4)-(5)) as $\mathbf{x}$ is updated during the optimization:

$$\mu_{DV}(\mathbf{x}) = \sum_{j=1}^{N_G} \mu_{DV_j}(\mathbf{x}) \approx \sum_{j=1}^{N_G} \left[\frac{1}{N_s} \sum_{i=1}^{N_s} \mu_{DV_j|EDP_j}(\mathbf{x}; \widetilde{edp}_j^{(i)}) \right] \tag{31}$$

$$\begin{aligned} \sigma_{DV}(\mathbf{x}) &= \sqrt{\sum_{j=1}^{N_G}\sum_{k=1}^{N_G} \sigma_{DV_j,DV_k}(\mathbf{x})} \\ &\approx \left\{ \sum_{j=1}^{N_G}\sum_{k=1}^{N_G} \left[\frac{\sum_{i=1}^{N_s} [\sigma_{DV_j,DV_k|EDP_j,EDP_k}(\mathbf{x}; \widetilde{edp}_j^{(i)}, \widetilde{edp}_k^{(i)})]}{N_s} \right. \right. \\ &\quad \left. \left. + \frac{\sum_{i=1}^{N_s} [\mu_{DV_j|EDP_j}(\mathbf{x}; \widetilde{edp}_j^{(i)}) - \mu_{DV_j}(\mathbf{x})] \cdot [\mu_{DV_k|EDP_k}(\mathbf{x}; \widetilde{edp}_k^{(i)}) - \mu_{DV_k}(\mathbf{x})]}{N_s - 1} \right] \right\}^{\frac{1}{2}} \end{aligned} \tag{32}$$

In practice, through Eqs. (31) and (32), each approximate demand sample is first used to estimate the conditional expectations and covariances of the group-level losses through the approaches of Sec. 3.3. Subsequently, the unconditional group-level loss statistics are estimated through Eqs. (6) and (7) in which the operations of expectation and covariance are carried out through the Monte Carlo estimators of Eqs. (8) and (9) and the N_s approximate demand samples. Equations (4) and (5) are then directly applied to estimate the searched after system-level loss statistics. Because the proposed approach is based on propagating approximate demand samples through the models of Sec. 3.3, it is termed a pseudo-simulation scheme. It should be highlighted that, through the proposed scheme, not only are the means and standard deviations of the individual group-level losses updated as $\mathbf{x}$ is varied, but also the correlations between the group-level losses.

4.2. Sub-Problem Formulation

Based on the approximation scheme introduced in the previous section, the following optimization sub-problem may be formulated and solved sequentially:

$$\begin{aligned}
&\text{Find} \quad \mathbf{x} = \{x_1, ..., x_N\}^T \\
&\text{to minimize} \quad V(\mathbf{x}) \\
&\text{subject to} \quad L(\mathbf{x}; im) \approx \widetilde{\mu}_{DV|IM}(\mathbf{x}; im) + \alpha \cdot \widetilde{\sigma}_{DV|IM}(\mathbf{x}; im) \leq \epsilon \\
&x_n \in \mathbb{X}_n^o \in \mathbb{X}_n \quad n = 1, \ldots, N
\end{aligned} \tag{33}$$

where $\widetilde{\mu}_{DV|IM}$ and $\widetilde{\sigma}_{DV|IM}$ are the approximations of $\mu_{DV|IM}$ and $\sigma_{DV|IM}$ through Eqs. (31)-(32), respectively; while $\mathbb{X}_n^o$ represents the search neighborhood of x_n defined by the minimum value, x_n^{min}, and maximum value, x_n^{max}, that x_n is allowed to take. These bounds are imposed in order to ensure the validity of the proposed approximation scheme. Because the optimal solution to Eq. (33) only satisfies the approximate performance constraint, the optimization sub-problem needs to be reformulated and solved again at the updated design point. This resolution process is termed a design cycle (DC) and needs to be repeated until solutions of two consecutive DCs meet a predefined convergence tolerances on the objective function. This ensures that the final solution is free of any approximations. In addition, as will be outlined in Sec. 4.2.1, the approximate statistics of Eqs. (31)-(32) allow for a direct calculation of the sensitivities with respect to $\mathbf{x}$ through the chain rule. Therefore, any gradient-based optimization algorithm can be used to efficiently solve the sub-problem of Eq. (33).

4.2.1. Sensitivities

The partial derivative of the approximate loss measure with respect to the nth element of the design variable vector, x_n, may be estimated as follows:

$$\frac{\partial L(\mathbf{x})}{\partial x_n} \approx \frac{\partial \widetilde{\mu}_{DV}(\mathbf{x})}{\partial x_n} + \alpha \cdot \frac{\partial \widetilde{\sigma}_{DV}(\mathbf{x})}{\partial x_n} \tag{34}$$

where the partial derivative of the approximate expected value of DV can be estimated through the chain rule as:

$$\frac{\partial \widetilde{\mu}_{DV}(\mathbf{x})}{\partial x_n} = \sum_{j=1}^{N_G} \left[\frac{1}{N_s} \sum_{i=1}^{N_s} \frac{\partial \mu_{DV_j|EDP_j}(\mathbf{x}; \widetilde{edp}_j^{(i)})}{\partial \widetilde{edp}_j^{(i)}} \cdot \frac{\partial \widetilde{edp}_j^{(i)}}{\partial x_n} \right] \tag{35}$$

where $\frac{\partial \mu_{DV_j|EDP_j}}{\partial \widetilde{edp}_j^{(i)}}$ denotes the partial derivative of the conditional expected group-level loss with respect to the approximate engineering demand sample, $\widetilde{edp}_j^{(i)}$, while $\frac{\partial \widetilde{edp}_j^{(i)}}{\partial x_n}$ is the partial derivative of $\widetilde{edp}_j^{(i)}$ with respect to x_n.

The partial derivative of the approximate standard deviation can also be calculated through the chain rule as:

$$\begin{aligned} \frac{\partial \widetilde{\sigma}_{DV}(\mathbf{x})}{\partial x_n} = & \Bigg\{ \sum_{j=1}^{N_G} \sum_{k=1}^{N_G} \Bigg[\sum_{i=1}^{N_s} \frac{1}{N_s} \Bigg(\frac{\partial \sigma_{DV_j,DV_k|EDP_j,EDP_k}(\mathbf{x}; \widetilde{edp}_j^{(i)}, \widetilde{edp}_k^{(i)})}{\partial \widetilde{edp}_j^{(i)}} \cdot \frac{\partial \widetilde{edp}_j^{(i)}}{\partial x_n} \\ & + \frac{\partial \sigma_{DV_j,DV_k|EDP_j,EDP_k}(\mathbf{x}; \widetilde{edp}_j^{(i)}, \widetilde{edp}_k^{(i)})}{\partial \widetilde{edp}_k^{(i)}} \cdot \frac{\partial \widetilde{edp}_k^{(i)}}{\partial x_n} \Bigg) \\ & + \sum_{i=1}^{N_s} \frac{1}{N_s - 1} \Bigg(\Bigg(\frac{\partial \mu_{DV_j|EDP_j}(\mathbf{x}; \widetilde{edp}_j^{(i)})}{\partial \widetilde{edp}_j^{(i)}} \cdot \frac{\partial \widetilde{edp}_j^{(i)}}{\partial x_n} - \frac{\partial \widetilde{\mu}_{DV_j}(\mathbf{x})}{\partial x_n} \Bigg) \\ & \cdot [\mu_{DV_k|EDP_k}(\mathbf{x}; \widetilde{edp}_k^{(i)}) - \mu_{DV_k}(\mathbf{x})] + [\mu_{DV_j|EDP_j}(\mathbf{x}; \widetilde{edp}_j^{(i)}) - \mu_{DV_j}(\mathbf{x})] \\ & \cdot \Bigg(\frac{\partial \mu_{DV_k|EDP_k}(\mathbf{x}; \widetilde{edp}_k^{(i)})}{\partial \widetilde{edp}_k^{(i)}} \cdot \frac{\partial \widetilde{edp}_k^{(i)}}{\partial x_n} - \frac{\partial \widetilde{\mu}_{DV_k}(\mathbf{x})}{\partial x_n} \Bigg) \Bigg) \Bigg] \Bigg\} \cdot \frac{1}{2 \cdot \widetilde{\sigma}_{DV}(\mathbf{x})} \end{aligned} \tag{36}$$

where $\frac{\partial \sigma_{DV_j,DV_k|EDP_j,EDP_k}}{\partial \widetilde{edp}_j^{(i)}}$ and $\frac{\partial \sigma_{DV_j,DV_k|EDP_j,EDP_k}}{\partial \widetilde{edp}_k^{(i)}}$ are the partial derivatives of the conditional covariance of group-level losses with respect to $\widetilde{edp}_j^{(i)}$ and $\widetilde{edp}_k^{(i)}$, respectively; $\frac{\partial \widetilde{\mu}_{DV_j}(\mathbf{x})}{\partial x_n}$ and

$\frac{\partial \widetilde{\mu}_{DV_k}(\mathbf{x})}{\partial x_n}$ are the partial derivatives of the approximate expected group-level losses with respect to x_n; while $\frac{\partial \widetilde{edp}_k^{(i)}}{\partial x_n}$ is the partial derivative of $\widetilde{edp}_k^{(i)}$ with respect to x_n. Derivation of $\frac{\partial \mu_{DV_j|EDP_j}}{\partial \widetilde{edp}_j^{(i)}}$, $\frac{\partial \widetilde{edp}_j^{(i)}}{\partial x_n}$, $\frac{\partial \sigma_{DV_j,DV_k|EDP_j,EDP_k}}{\partial \widetilde{edp}_j^{(i)}}$, and $\frac{\partial \widetilde{\mu}_{DV_j}(\mathbf{x})}{\partial x_n}$ can be found in Appendix D.

5. Numerical Applications

To illustrate the validity and applicability of the proposed approach, two case studies are presented in this section. The first is a small-scale case study that is considered with the aim of examining the validity of the proposed optimization strategy for solving ϵ-constraint problems. The second is a large-scale case study that is considered in order to illustrate the scalability of the proposed approach to practical problems involving hundreds of design variables and computationally burdensome numerical response models.

5.1. Small-scale Case Study

The goal of this case study is to identify the lateral load-resisting system of the two-story building outlined in Fig. 1 that minimizes the material volume, V, of the structural system while ensuring the satisfaction of a constraint on the loss measure, L, associated with an extreme wind scenario.

5.1.1. Description

The two-story building consists of two bays in the X-direction and four bays in the Y-direction, as shown in Fig. 1. The height of each story is 3.66 m, and the width of each bay is 7.62 m. Hence, the total height, total width, and total depth are 7.32 m, 15.24 m, and 30.48 m, respectively. It is of interest to design the structural system to help reduce the wind-induced responses in the X-direction. The load-resisting system is defined by two design variables that identify the size of the beams and columns within the system, as shown in Fig. 1(c). Both beams and columns are assumed to be square box sections defined by a mid-line diameter, $d_m \in [0.1 \text{ m}, 0.6 \text{ m}]$, and a wall thickness, $t_m = d_m/20$. For the initial design, all beams and columns are assigned with a mid-line diameter of 0.15 m. The resonant response is estimated based on the first two vibration modes which, for the initial design, have mean circular frequencies of $\omega_1 = 2.758$ rad/s and $\omega_2 = 8.020$ rad/s.

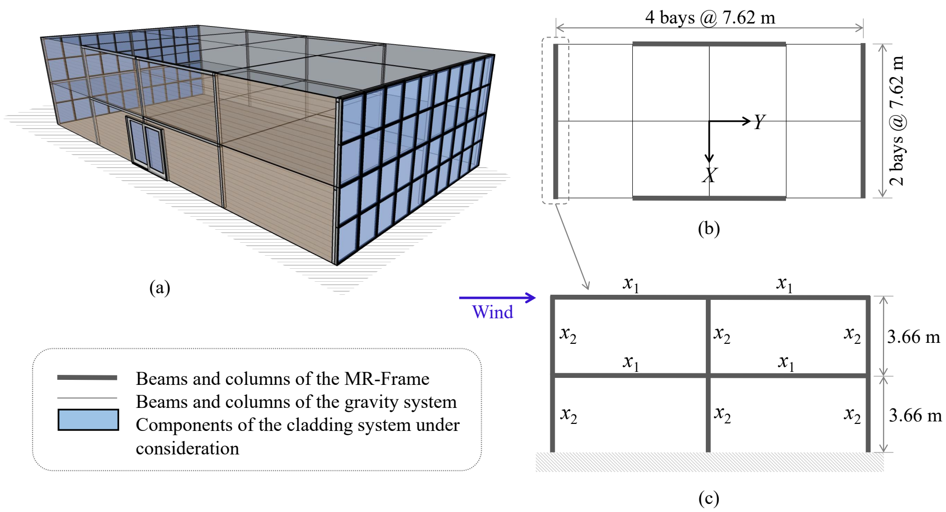

Figure 1: Two-story building system: (a) Isometric view, (b) Building plan, (c) Frame layout showing beam and column assignments.

The building is assumed to be located in Miami, Florida, USA, and is assigned to Risk Category II [26]. Hence, im is defined here in terms of the wind speed with a 700-year MRI, estimated from the wind speed dataset of the National Institute of Standards and Technology (NIST) associated with the Miami area of Florida [27]. In generating aerodynamic loads, the quasi-steady wind model outlined in [20, 28, 29] is adopted for simplicity.

The system-level performance is evaluated in terms of loss caused by damage to the midrise stick-built curtain wall of the building envelope. In particular, cladding components are susceptible to two sequential damage states, as reported in Table 1, where EDP_j are described in terms of the absolute maximum inter-story drift ratio in the plane of the cladding panels. Two PGs are identified with each group consisting of 40 components. Fragility curves with associated consequence functions were obtained from the fragility specification manager of the Federal Emergency Management Agency (FEMA) [19]. In modeling component correlations, the four trials summarized in Table 2 were considered, where Trial #1 and Trial #4 represent extreme cases: capacity and repair costs of components are assumed to be completely uncorrelated in Trial #1 and perfectly correlated in Trial #4. Regarding the partially correlated capacities in Trial #2 and #3, it is assumed that 70% of the total variance in the

Table 1: Parameters of the fragility and consequence functions in terms of repair cost. All functions are lognormal.

		Fragility Functions		Repair Cost	
DS	Description	μ_f	β_f	μ_c [$]	β_c
1	Glass cracking	0.021	0.45	2955	0.1185
2	Glass falling out	0.024	0.45	2955	0.1185

damage capacity is due to component capacity uncertainty, while the other 30% is due to engineering demand uncertainty. With respect to the component capacity uncertainty, 50% is assumed to be common to specific materials, 35% is common to specific component types and 15% is specific to each component. With respect to the demand uncertainty, 67% is assumed to be common to the entire structure, while 33% is common to a specific engineering demand parameter. These assumptions are consistent with those suggested in [17], and can be mathematically expressed for components m and n as [17]:

$$\rho_{lnC_{m,q},lnC_{n,r}} = 0.7\left(0.5\delta_{mat_m mat_n} + 0.35\delta_{type_m type_n} + 0.15\delta_{mn}\right) + 0.3\left(0.67 + 0.33\delta_{edp_m edp_n}\right) \tag{37}$$

where $\delta_{mat_m mat_n}$, $\delta_{type_m type_n}$, δ_{mn} and $\delta_{PG_m PG_n}$ are the Kronecker delta functions. In particular, $\delta_{mat_m mat_n} = 1$ if components m and n are made of the same material, $\delta_{type_m type_n} = 1$ if components m and n are of the same type, $\delta_{mn} = 1$ if $m = n$ (i.e. same component), $\delta_{PG_m PG_n} = 1$ if components m and n are in the same performance group; otherwise, $\delta_{mat_m mat_n}$, $\delta_{type_m type_n}$, δ_{mn} and $\delta_{PG_m PG_n}$ are equal to zero. The validation of the correlations considered in this study falls out side the scope of this work. However, this question would in general merit careful investigation and should be the focus of future studies.

To identify an optimal solution to the ϵ-constraint optimization problem, the threshold value ϵ was set to $100000, while $\alpha = 1$ was considered. A total of 20000 samples were used in the Monte Carlo simulation. The optimally criteria algorithm outlined in [30] was used to solve the sub-problems of Eq. (33), while the design variables were taken as continuous. The move limit on the design variables was set to $[x_n^{min}, x_n^{max}]=[x_n - 0.02, x_n + 0.02]$ m. The optimization is terminated when the relative change in the objective function between two consecutive DCs is less than 10^{-4}.

Table 2: Summary of the Trials #1 to #4.

		Correlations	
Trial #	Description	$\rho_{\ln C_{m,q},\ln C_{n,r}}$	$\rho_{DVC_m,DVC_n\|DS_m,DS_n}$
1	Uncorrelated capacity, uncorrelated cost	0	0
2	Partially correlated capacity, uncorrelated cost	0.9*	0
3	Partially correlated capacity, perfectly correlated cost	0.9*	1
4	Perfectly correlated capacity, perfectly correlated cost	1	1

*Based on the assumptions of Eq. (37).

5.1.2. Results and Discussion

From Fig. 2, which reports the convergence histories of the objective function for the four Trials, it is immediately evident that systems with higher component correlations require heavier, and therefore more costly, load-resisting systems to satisfy the predefined performance target. In particular, Trial #4 requires the most amount of material. Figure 3 shows the convergence histories of the two design variables in terms of the design cycle: all designs result in columns having a larger diameter than beams. Figures 2 and 3 shows that the optimal solutions of Trial #2 and Trial #3 are almost identical, which implies that, for this case study, the correlations between component repair costs, given the damage state, only minimally affect the final results.

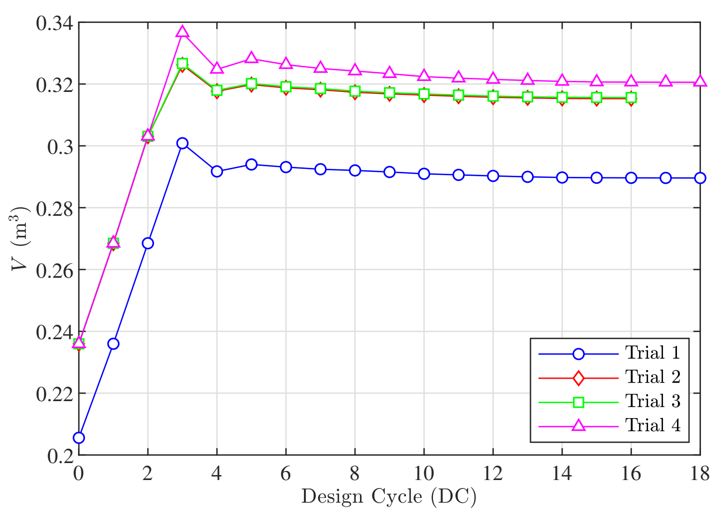

Figure 2: Convergence history of the objective function.

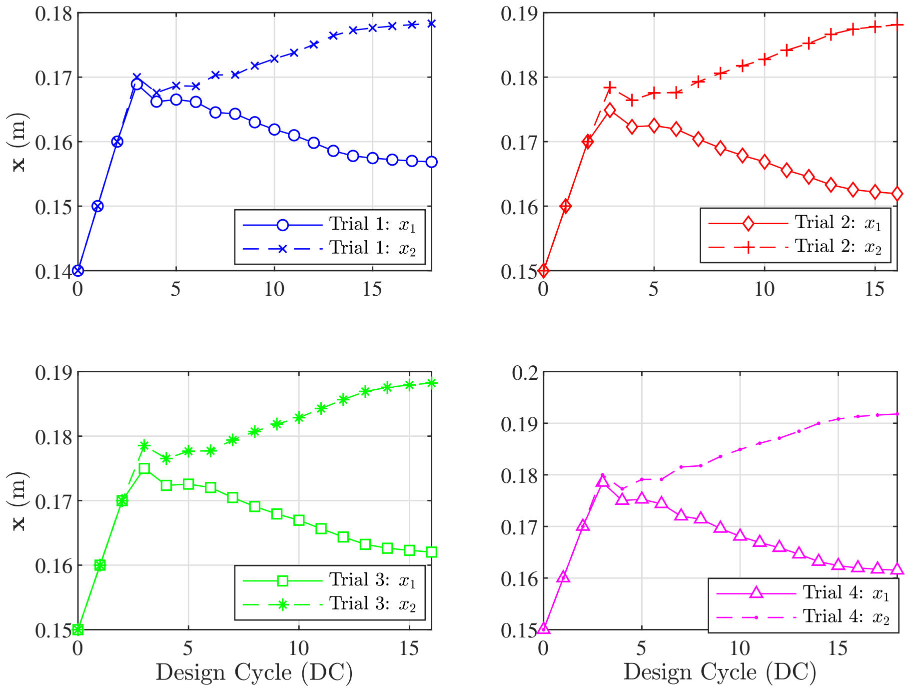

Figure 3: Convergence history of the design variables.

The effectiveness of the proposed method in solving the ϵ-constraint problem is demonstrated through Fig. 4, which shows the convergence histories of the constraint function, i.e. the loss measure L, of all trials. As can be seen, designs that satisfy the constraint were found in the first few design cycles, while the final solutions were efficiently obtained in less than 25 design cycles. In particular, the proposed approximation scheme demonstrates accuracy, as the approximations of L are very close to the estimations obtained from the Monte Carlo simulation at the end of each design cycle. In addition, Fig. 5 shows the convergence histories of the correlation coefficient between group losses in terms of the design cycle. It can be seen that the updating scheme for the correlations is also very effective. Figure 6 compares the reduced variates, g_1 and g_2, estimated in the initial and the final cycles. Values of g_1 and g_2 are seen to not change from the initial design to the final design: hence the assumption of constant reduced variates is acceptable, which is consistent with previous observations by the authors [20, 22].

To examine the validity of the proposed approach, the optimization problem of this case study was also solved without any approximation using the Genetic Algorithm (GA) of

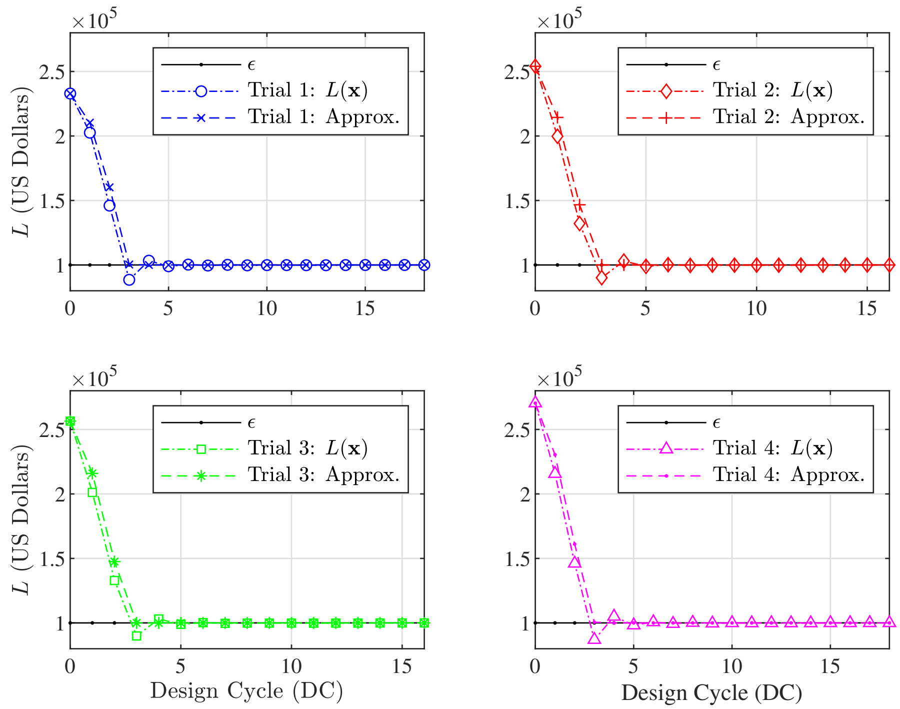

Figure 4: Convergence history of the constraint function L.

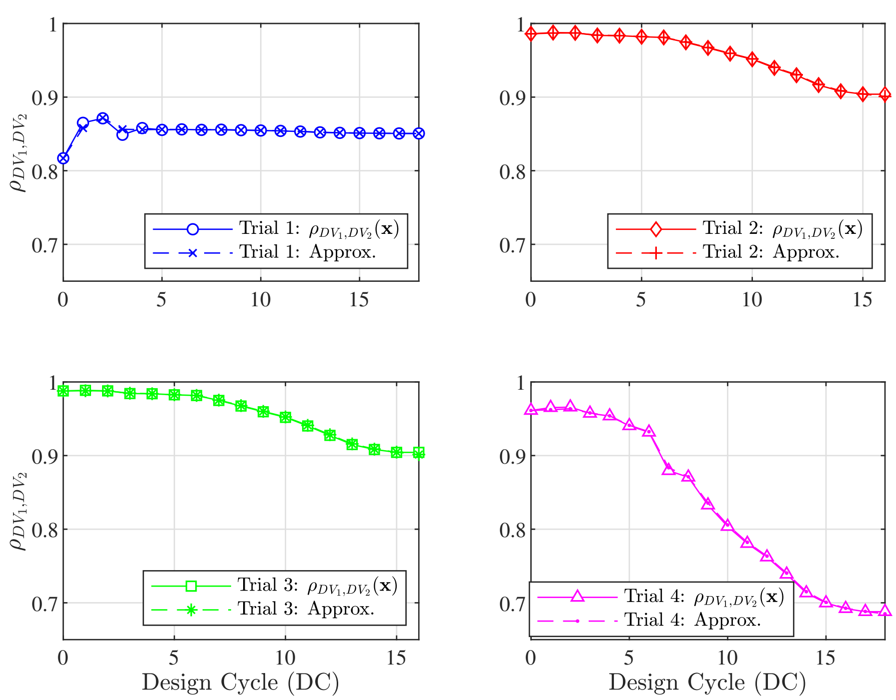

Figure 5: Convergence history of the correlation coefficient.

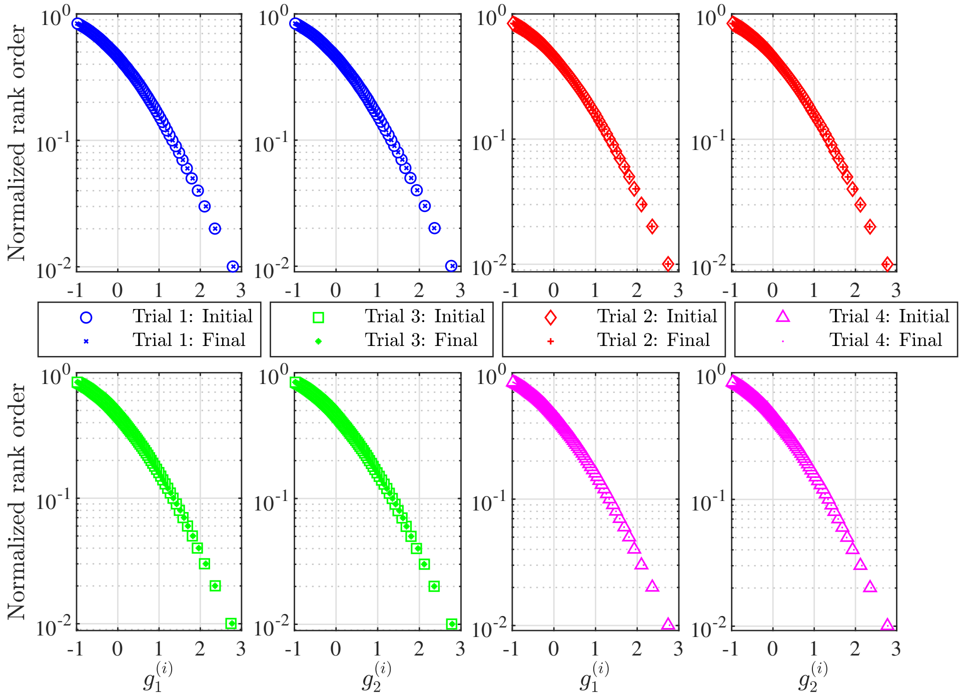

Figure 6: Convergence history of the reduced variates.

Matlab [31]. The final solutions obtained from both approaches are presented in Table 3. Both approaches identify solutions that satisfy the constraint while using near identical volumes of material. It can be observed that the solutions obtained from the GA are, at times, inferior to those obtained from the proposed approach (e.g. in Trial #3 it can be seen

Table 3: Summary of Results for Varied Component Correlations.

Trial	Approach	Final Design		Weight	Performance	CPU Time
		x_1	x_2	V	L	
1	Proposed	0.1569 m	0.1783 m	0.2896 m^3	$ 99983	232 s
	Genetic Algorithm	0.1551 m	0.1803 m	0.2895 m^3	$ 99991	84465 s
2	Proposed	0.1619 m	0.1881 m	0.3153 m^3	$ 99985	229 s
	Genetic Algorithm	0.1632 m	0.1867 m	0.3154 m^3	$ 99945	82266 s
3	Proposed	0.1620 m	0.1882 m	0.3156 m^3	$ 99982	252 s
	Genetic Algorithm	0.1392 m	0.2175 m	0.3258 m^3	$ 99984	92049 s
4	Proposed	0.1615 m	0.1918 m	0.3206 m^3	$ 99996	268 s
	Genetic Algorithm	0.1668 m	0.1862 m	0.3218 m^3	$ 99932	73027 s

that the GA approach led to a final design with higher material volume and loss). This can be traced back to how, as would be expected, GAs have a significantly slower convergence rate as compared to the proposed gradient-based approach. Therefore, if the same convergence criteria is set for both approaches (as in this case), GAs can lead to marginally inferior final solutions. Based on the same convergence criteria, the GA requires 80000-90000 seconds of CPU time, as compared to less than 300 seconds through the proposed approach. Therefore, the proposed approach not only finds, for all intents and purposes, an identical solution to that of the validated and approximation free GA scheme, but does so in over two orders of magnitude less computational time, highlighting the possibility of application to large-scale systems.

5.2. Large-scale Case Study

A large-scale case study is presented in this section to demonstrate the scalability of the proposed approach to design problems that involve a large number of design variables (e.g. in the order of hundreds or more structural members to be designed) as well as computationally burdensome numerical response models. While for the small-scale case study validation was carried out through direct comparison of the optimal solutions obtained from the proposed approach with those obtained through GAs, for the large-scale case study of this section this will not be carried out as the computational requirements of the GAs become prohibitive. With regard to the BODO applications, the goal of this case study is to identify a set of Pareto optimal designs that simultaneously minimize the structural material volume, V, and the loss measure, L, of the lateral load-resisting system outlined in Fig. 7.

5.2.1. Description

The building consists of 37 stories of which the first has a height of 6 m while all others have a height of 4 m. As shown in Fig. 7(a), the total width of five bays along the X-direction is 30 m, while the total width of six bays along the Y-direction is 60 m. The load-resisting system for wind loads acting in the X-direction is defined by a total of 259 design variables that identify the sizes of the beams and columns within the system. The numbering scheme used to locate each design variable is reported in Fig. 7(c). All beams are assumed to belong to the AISC (American Institute of Steel Construction) W24 family, while all columns are assumed to be square box sections with the mid-line diameter, d_m, belonging to the discrete set [0.20 m,0.25 m,...,3.95 m,4.00 m]. The wall thickness is again taken as $t_m = d_m/20$. For the initial design, all beams are set to a AISC W24 $\times$ 176 profile, while the mid-line diameter for all columns is set to d_m= 1.0 m. The resonant response is estimated based on the first three modes which have initial mean circular frequencies of $\omega_1 = 1.192$ rad/s, $\omega_2 = 3.750$ rad/s, $\omega_3 = 6.829$ rad/s.

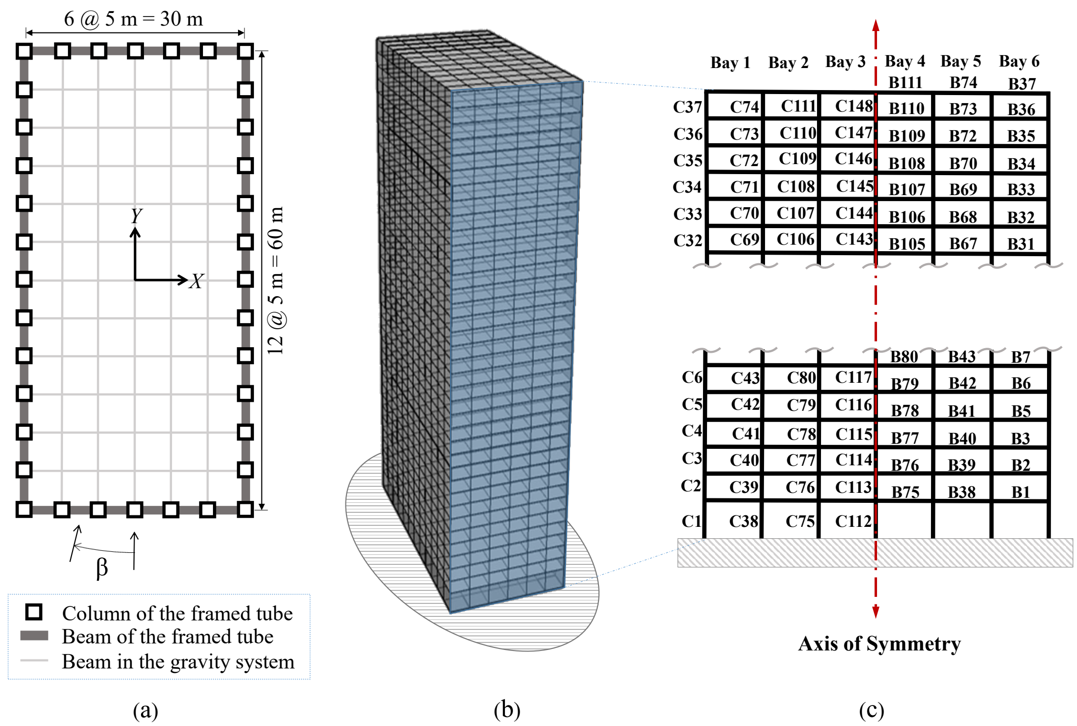

Figure 7: 37-story building system: (a) Building plan, (b) Isometric view, (c) Frame layout showing beam and column assignments.

The building is to be designed for Risk Category III [26], hence im is taken as the wind speed with a 1700-year MRI estimated from the NIST Miami hurricane wind speed dataset. In modeling the aerodynamic loads, the POD-based stochastic wind model is calibrated to wind tunnel datasets obtained from the Wind Pressure Database of the Tokyo Polytechnic University [32]. It should be noted that, in both case studies, the performance evaluation of the building system was carried out at wind intensities consistent with those suggested in the ASCE prestandard for performance-based wind design [33].

Similar to the previous case study, the system-level performance is evaluated in terms of loss to the building envelope that is assumed to be a midrise stick-built curtain wall. The two inter-story drift induced sequential damage states of Table 1 are again considered along with the associated fragility and consequence functions. In this case, a total of 37 PGs are identified with each group consisting of 80 components. In modeling component correlations, the four Trials outlined in Table 2 are once again considered.

To identify a set of Pareto optimal solutions, a series of five ϵ-constraint optimization problems were solved where the threshold values of ϵ were set to \$100000, \$250000, \$400000, \$700000, and \$1000000, while for robustness, a value of $\alpha = 2$ was considered. A total of 20000 samples were used in the Monte Carlo simulations. The discrete optimization algorithm outlined in [30] was used to solve the sub-problems of Eq. (33). The move limit, x_n^{min} and x_n^{max}, on the design variables was set to two sizes smaller and two sizes larger than the current sizes identified in $\mathbf{x}_{mc}$. The optimization stops when the relative change in the objective function between two consecutive DCs is less than or equal to 10^{-4}.

5.2.2. Results and Discussion

The set of Pareto optimal solutions, in the space of the two optimization objectives V and L, are presented in Fig. 8. The solid lines represent solutions obtained using the proposed pseudo-simulation approach, while the dashed line shows solutions obtained through the kriging-based approach outlined in [6]. It can be seen that in Trial #1 both approaches lead to consistent results in terms of the Pareto front, hence it is evident that the proposed approach is a valid alternative to the kriging-based approach. From all trials, it can be observed that, as expected, heavier designs perform better in resisting the wind loads and therefore result in lower losses, i.e. higher V leads to lower L. It is also important to note the significant impact that the assumption on correlation has on the optimal solutions. For any given value of L, systems with higher correlations between component capacities and correlations between component repair costs require 25-50% more investment in structural materials than systems whose components are uncorrelated. This can be traced back to how, as the component correlations increase, the variance of the total loss also increases.

Hence, to restrict the loss measure to a given value, building systems whose components are highly correlated require more structural material to help resist the wind action in order to reduce the structural demands, therefore reducing the expected loss and the variance that together make up the loss measure. Comparing the Pareto fronts of Trial #2 and Trial #3, solutions are very similar; hence correlations in the repair costs of cladding components, conditional on a set of damage states, do not seem to influence the susceptibility to loss of the system. Comparing Trial #2, Trial #3 and Trial #4, it can also be observed that the results are relatively similar (within 10% of each other) in terms of optimal material volume. A practical consequence of this observation is that, in cases where correlations in the component capacity are expected to be high (e.g. greater than 0.9), the assumption of full correlation may be made therefore avoiding the significant effort necessary for evaluating inter-component correlations. This practical result would seem to hold independently of the correlations between the repair costs.

Figure 9 reports the exceedance probability, $P(DV > L)$, of the system-level loss, DV, with respect to the loss threshold L. In particular, each point of Fig. 9 was estimated by carrying out an additional loss assessment in the final design point of each ϵ-constraint problem. In terms of structural design, the exceedance probabilities provide additional information that enrich the Pareto fronts of Fig. 8. Results in the form of Fig. 9 are particularly useful in providing trade-off information for decision-makers when choosing the optimal design that fits best their preferences. For example, as can be seen from Fig. 9, systems designed while accounting for component correlations, have in general lower exceedance probabilities than systems designed under the assumption of uncorrelated components. This is clearly evident from the comparison between the two extreme cases of Trial #1 and Trial #4, for which the neglect of correlations between the damage capacities and between the repair costs can lead to an order of magnitude increase in the exceedance probability. The impact of inter-component correlations seen in these results clearly highlights the need for optimal design frameworks that can treat correlations during the optimization process.

To examine the performance of the ϵ-constraint optimization strategy of Sec. 4, Fig. 10 shows the convergence histories of the material volume in terms of the design cycles for the optimal designs associated with $L \leq \$400000$ (i.e. #3, #8, #13 and #18). As can be seen,

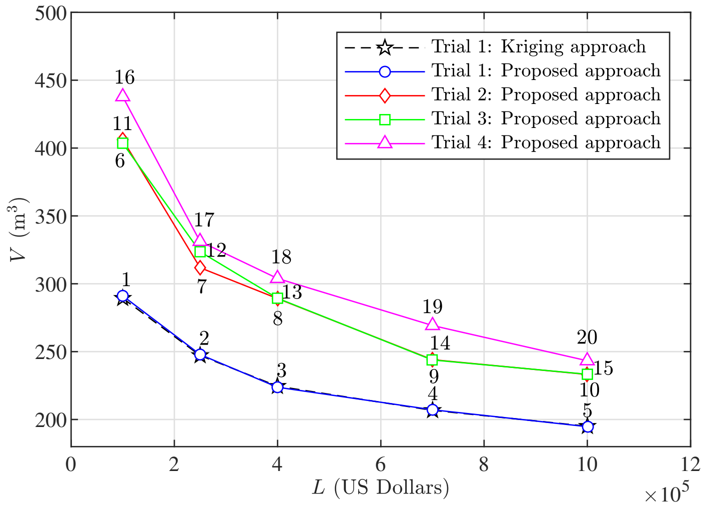

Figure 8: Pareto front of material volume vs loss measure for the 37-story system.

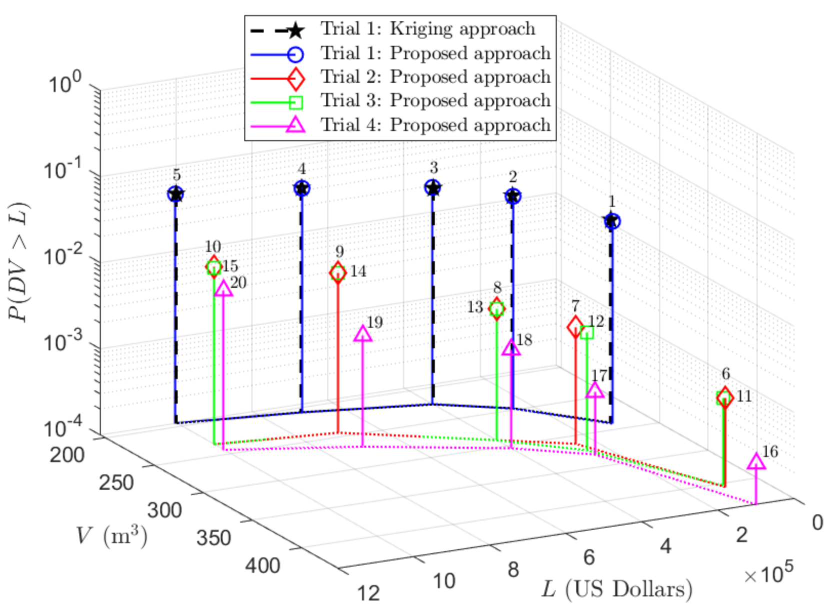

Figure 9: Pareto front of the objective functions with associated exceedance probability.

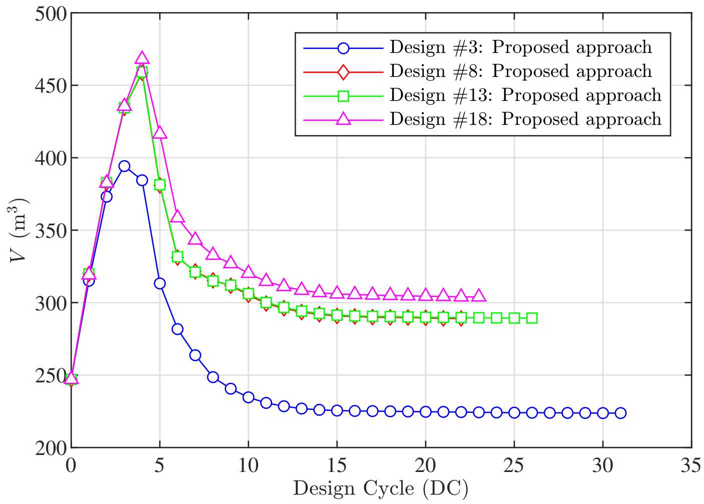

Figure 10: Convergence history of the objective function, V, for designs #3,#8,#13,#18.

smooth and steady convergence is seen for all cases. With respect to wind-induced losses, Fig. 11 illustrates the corresponding convergence histories of the loss measure obtained through the proposed approach. Simialr to the small-scale case study, the approximation scheme of Sec. 4 is seen to effectively provide accurate loss estimation during the optimization. In particular, designs that satisfy the system-level loss constraint were obtained within five design cycles with the later cycles serving to furhter minimize V. These results clearly highlights the effectiveness of the proposed method. Similar results were observed when solving all of the ϵ-constraint problems. A major advantage of the proposed method over existing methods (e.g. the kriging-based approach of [6]) is that it allows the correlation between group-level losses to be modeled and updated during the optimization process. Figure 12 shows an example of the convergence histories of the correlation coefficient between group-level losses associated with cladding components on floor 15 and floor 20 of the building (i.e. DV_{15} and DV_{20}). It can be observed that the correlations will in general change during each design cycle, especially in the early stages of finding designs that satisfy the constraint. As illustrated in Fig. 12, these changes were effectively approximated through the proposed scheme of Sec. 4.1.

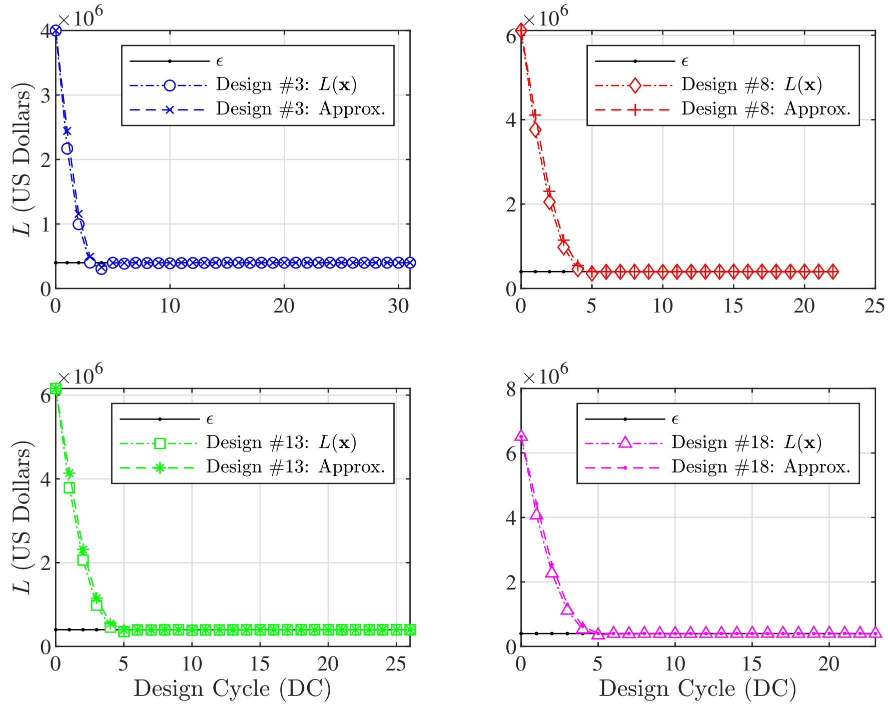

Figure 11: Convergence history of the objective function, L, for for designs #3,#8,#13,#18.

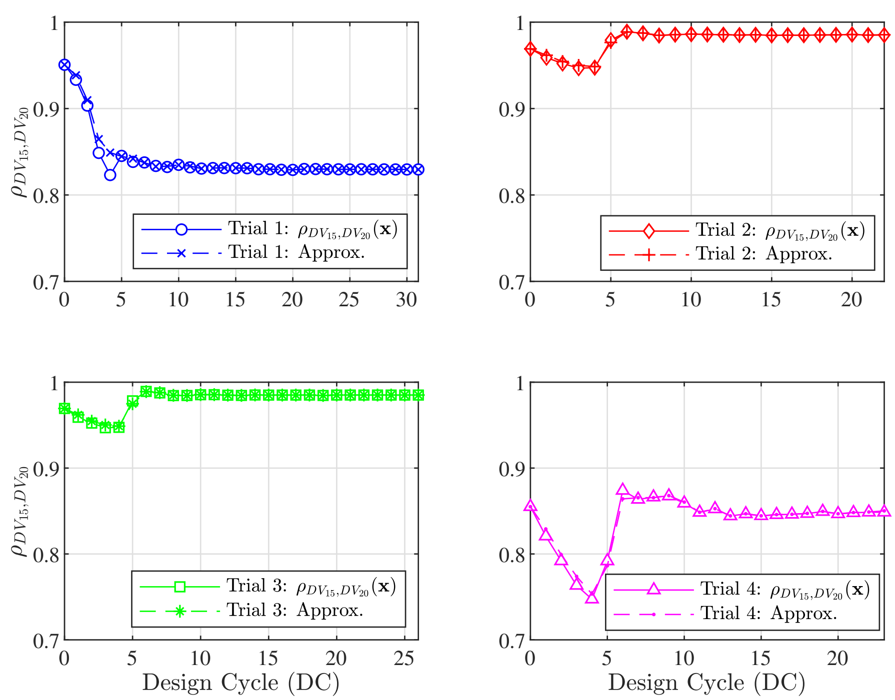

Figure 12: Convergence history of the correlation coefficient between DV_{15} and DV_{20} for designs #3,#8,#13,#18.

6. Conclusions

This paper presented a design optimization approach that can explicitly account for inter-component correlations in the performance assessment and optimization of wind-excited building systems. The proposed approach integrates bi-objective design optimization schemes with probabilistic performance-based wind engineering methodologies. In modeling the system performance under the action of stochastic wind loads, a loss measure is defined in terms of the expected value and variance of the system-level loss. Through the concept of fragility, closed-form functions were derived that relate samples of engineering demands to the second order statistics of the system-level loss while explicitly treating correlations between both the component capacities and the component losses. Through the ϵ-constraint approach, a bi-objective design optimization scheme was formulated for simultaneously minimizing the initial cost of the structure and the anticipated future losses caused by wind induced damage. For solving each ϵ-constraint problem, a strategy is proposed that centers on formulating and solving a sequence of decoupled approximate sub-problems that are constructed from approximate demand samples estimated from an augmented simulation carried out in the solution of the previous sub-problem. The approximate demand samples are used to estimate the second-order statistics of the wind-induced losses through the derived closed-form relationships and a pseudo-simulation scheme. The availability of the sensitivities with respect to the design variables enables the use of efficient gradient based optimization schemes for solving each sub-problems. The effectiveness of the proposed method and its scalability to high-dimensional problems were illustrated through the optimal design of two moment-resisting frames of building systems subject to stochastic wind loads. It was observed that designs that do not account for inter-component correlations run the risk of being significantly underdesigned. This finding highlights the need for methods, such as the one outlined in this work, that allows inter-component correlations to be modeled and updated throughout the design optimization process.

7. Acknowledgments

This research effort was in part supported by the National Science Foundation (NSF) under Grant No. CMMI-1750339. This support is gratefully acknowledged.

Appendix A. Estimation of Resonant Modal Response

This appendix outlines the procedure used to estimate a sample of the resonant modal response vector associated with the first M modes, $\mathbf{q}_{R_M}(t)$, which is needed for estimating a sample of the response process, $r_j^{(i)}(t)$ of Eq. (11) of Sec. 3.2.

To estimate the resonant modal response, the following equations of motion must first be solved through a modal analysis framework:

$$\mathbf{m}\ddot{\mathbf{q}}(t,\mathbf{u})+\mathbf{c}\dot{\mathbf{q}}(t,\mathbf{u})+\mathbf{k}\mathbf{q}(t,\mathbf{u})=\mathbf{\Phi}_M^T\mathbf{f}(t,\mathbf{u}) \tag{A.1}$$

where $\mathbf{q}(t)$, $\dot{\mathbf{q}}(t)$ and $\ddot{\mathbf{q}}(t)$ are the vector-valued generalized displacement, velocity and acceleration response processes respectively; $\mathbf{\Phi}_M=[\boldsymbol{\phi}_1,...,\boldsymbol{\phi}_M]$ is the mode shape matrix of order M; while $\mathbf{m}$, $\mathbf{c}$, and $\mathbf{k}$ are generalized mass, damping, and stiffness matrices respectively. The mth component of $\mathbf{m}$, $\mathbf{c}$, and $\mathbf{k}$ can be estimated as:

$$\begin{aligned}
m_m &= \phi_m^T\mathbf{M}\phi_m \\
c_m &= 2m_m s_{3_m}\zeta_m s_{2_m}\omega_m \\
k_m &= m_m(s_{2_m}\omega_m)^2
\end{aligned} \tag{A.2}$$

where ω_m is the mth natural frequency and ζ_m is the generalized damping ratio associated with the mth mode; S_{2_m} is an uncertain parameter associated with the variability in the estimate of ω_m while S_{3_m} is an uncertain parameter modeling the variability associated with the value of ζ_m. In this work, S_{2_m} and S_{3_m} are to be considered components of the random vector $\mathbf{U}$.

By solving Eq. (A.1), the total modal response associated with the mth mode, $q_m(t)$, can be determined and used to estimate the mth component of $\mathbf{q}_{R_M}(t)$ as:

$$q_{R_m}(t,\mathbf{u}) = q_m(t,\mathbf{u}) - q_{B_m}(t,\mathbf{u}) \tag{A.3}$$

where the background modal response, q_{B_m}, is given by:

$$q_{B_m}(t,\mathbf{u}) = \frac{1}{(s_{2_m}\omega_m)^2}\boldsymbol{\phi}_m^T\mathbf{f}(t,\mathbf{u}) \tag{A.4}$$

Appendix B. POD-Based Stochastic Wind Model

This appendix outlines the procedure used to simulate a sample of the aerodynamic loads, $\mathbf{f}(t)$, needed for estimating the stochastic response process, $r_j^{(i)}(t)$ of Eq. (11) of Sec. 3.2.

To ensure that the vector-valued stochastic process, $\mathbf{f}(t)$, includes complex phenomena such as vortex shedding, wind tunnel data is used to calibrate a proper orthogonal decomposition (POD) [23] based spectral representation model. Following this data-driven aerodynamic POD approach, each component of $\mathbf{f}(t)$ can be simulated as:

$$\mathrm{f}_j(t;\bar{v}_H,\beta) = \sum_{l=1}^{N_l}\sum_{n_1=1}^{N_{n_1}-1}\Bigg\{2|\Psi_{jl}(\omega_{n_1};\beta)|\sqrt{\Lambda_l(\omega_{n_1};\bar{v}_H,\beta)\Delta\omega} \cdot \cos(\omega_{n_1}t+\vartheta_{jl}(\omega_{n_1};\beta)+\theta_{n_1 l})\Bigg\} \tag{B.1}$$

where N_l is the total number of loading modes considered in the model; $\Delta\omega$ is the frequency increment (accordingly, the Nyquist frequency is $N_{n_1}\Delta\omega/2$, with N_{n_1} the total number of discrete frequencies considered), while $\omega_{n_1} = n_1\Delta\omega$; $\theta_{n_1 l}$ is an independent random variable characterizing the stochastic nature of the wind, uniformly distributed over $[0, 2\pi]$ and collected in the uncertain vector $\mathbf{U}$; $\vartheta_{jl} = \tan^{-1}(\mathbf{Im}(\Upsilon_{jl})/\mathbf{Re}(\Upsilon_{jl}))$; while $\Upsilon_{jl}(\omega)$ and $\Lambda_l(\omega)$ are components of $\Upsilon(\omega)$ and $\Lambda(\omega)$ obtained from the nontrivial solution of the following eigenvalue problem:

$$[\mathbf{S}_f(\omega;\bar{v}_H,\beta) - \Lambda(\omega;\bar{v}_H,\beta)\mathbf{I}]\Upsilon(\omega;\beta) = 0 \tag{B.2}$$

where $\mathbf{S}_f$ is the cross power spectral density matrix of the wind tunnel estimated aerodynamic load processes. Since Λ can be scaled to different wind speeds after Λ and Υ are estimated at wind tunnel speed, Eq. (B.2) does not need to be solved for each wind speed, $\bar{v}_H$, of interest.

The site-specific wind speed at the top of the building, $\bar{v}_H$, is obtained from the wind speed data measured at nearby meteorological stations. In particular, from this data, a mean wind speed–$\bar{v}_y$–of averaging time τ and mean recurrence interval (MRI) y years, can be extracted. This wind speed is here assumed as the intensity measure (im). In this work, the corresponding site-specific wind speed $\bar{v}_H$, averaged over a time interval T, can then be obtained through the following transformation [34]:

$$\bar{v}_H(T, z_0) = e_7 e_3(\tau, T) \left(\frac{e_5 z_0}{e_6 z_{01}}\right)^{e_4 \delta} \frac{\ln[H/(e_5 z_0)]}{\ln[H_{met}/(e_6 z_{01})]} e_2 e_1 \bar{v}_y(\tau, H_{met}, z_{01}) \tag{B.3}$$

where $\delta = 0.0706$ is an empirical constant, while e_1 to e_7 are random parameters modeling the uncertainties affecting the model. In particular, e_1 and e_2 account for observational and sampling errors in $\bar{v}_y$; $e_3(\tau, T)$ is a random conversion factor that accounts for the uncertainty in converting between the wind speed averaging times τ and T; e_4, e_5, and e_6 are random variables modeling the uncertainties with respect to the actual values of δ and of the roughness lengths z_0 and z_{01}; while e_7 is a model uncertainty parameter to be used in the case that the transformation of Eq. (B.3) is used for modeling hurricane winds. These uncertain parameters E_1-E_7 are to be considered components of the random vector **U**. Possible marginal distributions for the elements of **U** can be found in Table B.4

Table B.4: Marginal distributions for the elements of the uncertain vector **U**.

Variable	Mean	CV	Distribution	Ref.
S_1	1	0.025	Trunc. Normal	[34]
$S_{2_i}*$	1	0.3	Lognormal	[35]
$S_{3_i}*$	1	0.01	Lognormal	[35]
$\theta_{n_1 l} **$	π	$\frac{2}{\sqrt{12}}$	uniform	[29]
E_1	1	0.1	Trunc. Normal	[34]
E_2	1	0.025	Normal	[36]
E_3	$***$	0.075	Normal	[36]
E_4	1	0.1	Trunc. Normal	[36]
E_5	1	0.3	Trunc. Normal	[36]
E_6	1	0.3	Trunc. Normal	[36]
E_7	1	0.05	Normal	[36]

* for $i = 1, \ldots, m$

$**$ for $l = 1, \ldots, N_l$ and $n_1 = 1, \ldots, (N_{n_1} - 1)$

$***$ Dependent on averaging times τ and T

Appendix C. Derivation of the Conditional Expectation

This appendix provides detailed derivation of Eq. (17), which is necessary for the estimation of the conditional covariance between group-level losses of Sec. 3.3.2.

The conditional expected value of the product of DVC_{jm} and DVC_{kn}, as shown in Eq. (17), can be estimated through the concept of total probability as:

$$
\begin{aligned}
&\mu_{DVC_{jm}DVC_{kn}|EDP_j,EDP_k}(edp_j^{(i)}, edp_k^{(i)}) \\
&= \sum_{q=1}^{N_{DS_m}} \sum_{r=1}^{N_{DS_n}} \left[\mu_{DVC_{jm}DVC_{kn}|DS_m,DS_n}(q,r) \cdot \mathrm{P}_{DS_m,DS_n|EDP_j,EDP_k}(q,r|edp_j^{(i)}, edp_k^{(i)})\right] \\
&= \sum_{q=1}^{N_{DS_m}} \sum_{r=1}^{N_{DS_n}} \Big[\Big(\sigma_{DVC_{jm}DVC_{kn}|DS_m,DS_n}(q,r) + \mu_{DVC_{jm}|DS_m}(q) \cdot \mu_{DVC_{kn}|DS_n}(r)\Big) \\
&\qquad \cdot \mathrm{P}_{DS_m,DS_n|EDP_j,EDP_k}(q,r|edp_j^{(i)}, edp_k^{(i)})\Big] \\
&= \sum_{q=1}^{N_{DS_m}} \sum_{r=1}^{N_{DS_n}} \Big[\Big(\rho_{DVC_{jm},DVC_{kn}|DS_m,DS_n}(q,r) \cdot \sigma_{DVC_{jm}|DS_m}(q) \cdot \sigma_{DVC_{kn}|DS_n}(r) \\
&\qquad + \mu_{DVC_{jm}|DS_m}(q) \cdot \mu_{DVC_{kn}|DS_n}(r)\Big) \cdot \mathrm{P}_{DS_m,DS_n|EDP_j,EDP_k}(q,r|edp_j^{(i)}, edp_k^{(i)})\Big]
\end{aligned}
\tag{C.1}
$$

where $\mu_{DVC_{jm}DVC_{kn}|DS_m,DS_n}(q,r)$ is the expected value of the product of DVC_{jm} and DVC_{kn} conditioned on the damage states q and r; $\mathrm{P}_{DS_m,DS_n|EDP_j,EDP_k}$ is the conditional joint probability of the mth and the nth component damage state given EDP_j and EDP_k; $\sigma_{DVC_{jm}DVC_{kn}|DS_m,DS_n}(q,r)$ is the variance of the product of DVC_{jm} and DVC_{kn} conditioned on the damage state q and r; $\mu_{DVC_{jm}|DS_m}(q)$ and $\mu_{DVC_{kn}|DS_n}(r)$ are the means of DVC_{jm} and DVC_{kn} conditioned on the damage state q and r; $\rho_{DVC_{jm},DVC_{kn}|DS_m,DS_n}(q,r)$ is the correlation between the mth and the nth component losses due to the damage states q and r; while $\sigma_{DVC_{jm}|DS_m}(q)$ and $\sigma_{DVC_{kn}|DS_n}(r)$ are the standard deviations of DVC_{jm} and DVC_{kn} conditioned on the damage states q and r.

Appendix D. Details on the Sensitivity Estimation

This appendix provides detailed derivations of $\frac{\partial \mu_{DV_j|EDP_j}}{\partial \widetilde{edp}_j^{(i)}}$, $\frac{\partial \widetilde{edp}_j^{(i)}}{\partial x_n}$, $\frac{\partial \sigma_{DV_j,DV_k|EDP_j,EDP_k}}{\partial \widetilde{edp}_j^{(i)}}$, and $\frac{\partial \widetilde{\mu}_{DV_j}(\mathbf{x})}{\partial x_n}$, which are necessary for the estimation of the partial derivatives of the approximate expected value and standard deviation of the loss measure of Sec. 4.2.1.

The partial derivative of the expected group-level loss in Eq. (36) with respect to the design variable can be estimated as follow:

$$\frac{\partial \widetilde{\mu}_{DV_j}(\mathbf{x})}{\partial x_n} = \frac{1}{N_s} \sum_{i=1}^{N_s} \frac{\partial \widetilde{\mu}_{DV_j|EDP_j}(\mathbf{x}; \widetilde{edp}_j^{(i)})}{\partial \widetilde{edp}_j^{(i)}} \cdot \frac{\partial \widetilde{edp}_j^{(i)}}{\partial x_n} \tag{D.1}$$

where the partial derivative of the conditional expected group-level loss and can be estimated as:

$$\frac{\partial \widetilde{\mu}_{DV_j|EDP_j}(\mathbf{x}; \widetilde{edp}_j^{(i)})}{\partial \widetilde{edp}_j^{(i)}} = \sum_{m=1}^{N_{C_j}} \frac{\partial \widetilde{\mu}_{DVC_{jm}|EDP_j}(\mathbf{x}; \widetilde{edp}_j^{(i)})}{\partial \widetilde{edp}_j^{(i)}} \tag{D.2}$$

where the partial derivative of the conditional expected component loss can be estimated as:

$$\frac{\partial \widetilde{\mu}_{DVC_{jm}|EDP_j}(\mathbf{x}; \widetilde{edp}_j^{(i)})}{\partial \widetilde{edp}_j^{(i)}} = \sum_{q=0}^{N_{DS_m}} \mu_{DVC_{jm}|DS_m}(q) \cdot \left[\frac{\partial \mathrm{Fr}_q(\widetilde{edp}_j^{(i)})}{\partial \widetilde{edp}_j^{(i)}} - \frac{\partial \mathrm{Fr}_{q+1}(\widetilde{edp}_j^{(i)})}{\partial \widetilde{edp}_j^{(i)}} \right] \tag{D.3}$$

where the derivative of the fragility functions results in the probability density function of the corresponding distribution.

The partial derivative of the approximate demand sample in Eqs. (35)-(36) with respect to the nth component of the design variable vector may be estimated through the following scheme:

$$\frac{\partial \widetilde{edp}_j^{(i)}(\mathbf{x})}{\partial x_n} = \frac{\partial \mathbf{\Gamma}_j^T(\mathbf{x})}{\partial x_n} \bar{\mathbf{\Psi}}_j(\mathbf{x}_{mc}) + g_j^{(i)}(\mathbf{x}_{mc}) \cdot \frac{\partial \mathbf{\Gamma}_j^T(\mathbf{x})}{\partial x_n} \hat{\mathbf{\Psi}}_j(\mathbf{x}_{mc}) \tag{D.4}$$

where $\frac{\partial \mathbf{\Gamma}_j^T}{\partial x_n}$ is the derivatives of the influence functions Γ_j with respect to x_n and can be efficiently estimated through traditional approaches [30, 37].

The partial derivative of the conditional covariance between group-level losses in Eq. (36) with respect to the approximate engineering demand sample can be estimated as follow:

$$\begin{aligned} &\frac{\partial \widetilde{\sigma}_{DV_j,DV_k|EDP_j,EDP_k}(\mathbf{x}; \widetilde{edp}_j^{(i)}, \widetilde{edp}_k^{(i)})}{\partial \widetilde{edp}_j^{(i)}} \\ &= \sum_{m=1}^{N_{C_j}} \sum_{n=1}^{N_{C_k}} \Bigg[\frac{\partial \widetilde{\rho}_{DVC_{jm},DVC_{kn}|EDP_j,EDP_k}(\widetilde{edp}_j^{(i)}, \widetilde{edp}_k^{(i)})}{\partial \widetilde{edp}_j^{(i)}} \cdot \widetilde{\sigma}_{DVC_{jm}|EDP_j}(\widetilde{edp}_j^{(i)}) \cdot \widetilde{\sigma}_{DVC_{kn}|EDP_k}(\widetilde{edp}_k^{(i)}) \\ &\qquad + \widetilde{\rho}_{DVC_{jm},DVC_{kn}|EDP_j,EDP_k}(\widetilde{edp}_j^{(i)}, \widetilde{edp}_k^{(i)}) \cdot \frac{\partial \widetilde{\sigma}_{DVC_{jm}|EDP_j}(\widetilde{edp}_j^{(i)})}{\partial \widetilde{edp}_j^{(i)}} \cdot \widetilde{\sigma}_{DVC_{kn}|EDP_k}(\widetilde{edp}_k^{(i)}) \Bigg] \end{aligned} \tag{D.5}$$

where the partial derivative of the conditional correlation coefficient, as defined in Eq. (16), may be estimated through the quotient rule, while the following derivatives are needed (in addition to $\frac{\partial \widetilde{\mu}_{DVC_{jm}|EDP_j}}{\partial \widetilde{edp_j}^{(i)}}$):

$$\begin{aligned}
&\frac{\partial \widetilde{\sigma}_{DVC_{jm}|EDP_j}(\widetilde{edp_j}^{(i)})}{\partial \widetilde{edp_j}^{(i)}} \\
&= \frac{1}{2 \cdot \widetilde{\sigma}_{DVC_{jm}|EDP_j}(\widetilde{edp_j}^{(i)})} \cdot \Bigg[\sum_{q=0}^{N_{DS}^m} \sigma^2_{DVC_{jm}|DS_m}(q) \cdot \left(\frac{\partial \mathrm{Fr}_q(\widetilde{edp_j}^{(i)})}{\partial \widetilde{edp_j}^{(i)}} - \frac{\partial \mathrm{Fr}_{q+1}(\widetilde{edp_j}^{(i)})}{\partial \widetilde{edp_j}^{(i)}} \right) \\
&\quad + \sum_{q=0}^{N_{DS}^m} (\mu_{DVC_{jm}|DS_m}(q) - \widetilde{\mu}_{DVC_{jm}|EDP_j}(\widetilde{edp_j}^{(i)}))^2 \cdot \left(\frac{\partial \mathrm{Fr}_q(\widetilde{edp_j}^{(i)})}{\partial \widetilde{edp_j}^{(i)}} - \frac{\partial \mathrm{Fr}_{q+1}(\widetilde{edp_j}^{(i)})}{\partial \widetilde{edp_j}^{(i)}} \right) \\
&\quad + \sum_{q=0}^{N_{DS}^m} 2 \cdot (\mu_{DVC_{jm}|DS_m}(q) - \widetilde{\mu}_{DVC_{jm}|EDP_j}(edp_j^{(i)})) \cdot \left(- \frac{\partial \widetilde{\mu}_{DVC_{jm}|EDP_j}(\widetilde{edp_j}^{(i)})}{\partial \widetilde{edp_j}^{(i)}} \right) \\
&\qquad \cdot \left(\mathrm{Fr}_q(\widetilde{edp_j}^{(i)}) - \mathrm{Fr}_{q+1}(\widetilde{edp_j}^{(i)}) \right) \Bigg]
\end{aligned} \tag{D.6}$$

$$\frac{\partial \mathrm{Fr}_{DS_m,DS_n|EDP_j,EDP_k}(q,r|edp_j^{(i)},edp_k^{(i)})}{\partial \widetilde{edp_j}^{(i)}} = \frac{\partial \mathrm{P}(\ln C_{m,q} < \ln edp_j^{(i)}, \ln C_{n,r} < \ln edp_k^{(i)})}{\partial \widetilde{edp_j}^{(i)}} \tag{D.7}$$

where the derivative of the joint cumulative distribution function results in the joint probability density function of the corresponding distribution.

References

[1] Liu, M., Frangopol, D.M.. Optimizing bridge network maintenance management under uncertainty with conflicting criteria: Life-cycle maintenance, failure, and user costs. J Struct Eng 2006;132(11):18351845.

[2] Frangopol, D.M.. Life-cycle performance, management, and optimisation of structural systems under uncertainty: accomplishments and challenges. Struct Infrastruct Eng 2011;7(6):389413.

[3] Gidaris, I., Taflanidis, A.A., Lopez-Garcia, D., Mavroeidis, G.P.. Multiobjective riskinformed design of floor isolation systems. Earthq Eng Struct Dyn 2016;45:12931313.

[4] Byun, J.E., Song, J.. Efficient optimization for multi-objective decision-making on civil systems using discrete influence diagram. In: 13th International Conference on Applications of Statistics and Probability in Civil Engineering (ICASP13). Seoul, South Korea; 2019,.

[5] Taflanidis, A.A., Giaralis, A., Patsialis, D.. Multi-objective optimal design of inerter-based vibration absorbers for earthquake protection of multi-storey building structures. J Franklin Inst 2019;356(14):7754–7784.

[6] Suksuwan, A., Spence, S.M.J.. Performance-based bi-objective design optimization of wind-excited building systems. J Wind Eng Ind Aerodyn 2019;190:40–52.

[7] Byun, J.E., Song, J.. Efficient probabilistic multi-objective optimization of complex systems using matrix-based bayesian network. Reliab Eng Syst Saf 2020;200(106899).

[8] Ciampoli, M., Petrini, F., Augusti, G.. Performance-Based Wind Engineering: Towards a general procedure. Struct Saf 2011;33(6):367–378.

[9] Petrini, F., Ciampoli, M.. Performance-based wind design of tall buildings. Struct Infrastruct Eng 2012;8(10):954–966.

[10] Caracoglia, L.. A stochastic model for examining along-wind loading uncertainty and intervention costs due to wind-induced damage on tall buildings. Eng Struct 2014;78:121–132.

[11] Beck, A.T., Kougioumtzoglou, I.A., dos Santos, K.R.M.. Optimal performance-based design of non-linear stochastic dynamical RC structures subject to stationary wind excitation. Eng Struct 2014;78:145–153.

[12] Chuang, W., Spence, S.M.J.. A performance-based design framework for the integrated collapse and non-collapse assessment of wind excited buildings. Eng Struct 2017;150:746–758.

[13] Cui, W., Caracoglia, L.. A unified framework for performance-based wind engineering of tall buildings in hurricane-prone regions based on lifetime intervention-cost estimation. Struct Saf 2018;73:75–86.

[14] Ouyang, Z., Spence, S.M.J.. A performance-based wind engineering framework for the envelope system of engineered buildings subject to directional wind and rain hazards. J Struct Eng 2019;.

[15] Cui, W., Caracoglia, L.. Performance-based wind engineering of tall buildings examining life-cycle downtime and multisource wind damage. J Struct Eng 2020;146(1).

[16] Baker, J.W., Cornell, C.A.. Uncertainty specification and propagation for loss estimation using FOSM method. Pacific Earthquake Engineering Research Center; 2003.

[17] Bradley, B.A., Lee, D.S.. Component correlations in structure-specific seismic loss estimation. Earthq Eng Struct Dyn 2010;39(3):237–258.

[18] Aslani, H.. Probabilistic earthquake loss estimation and loss disaggregation in buildings. Ph.D. thesis; John A. Blume Earthquake Engineering Centre, Department of Civil and Environmental Engineering; Stanford University; 2005.

[19] Federal Emergency Management Agency (FEMA), . Seismic performance assessment of buildings, Volume 1 Methodology (FEMA Publication P-58-1). Washington, DC; 2012.

[20] Suksuwan, A., Spence, S.M.J.. Performance-based design optimization of uncertain wind excited systems under system-level loss constraints. Struct Saf 2019;80:13–31.

[21] Spence, S.M.J., Kareem, A.. Performance-based design and optimization of uncertain wind-excited dynamic building systems. Eng Struct 2014;78:133–144.

[22] Suksuwan, A., Spence, S.M.J.. Optimization of uncertain structures subject to stochastic wind loads under system-level first excursion constraints: A data-driven approach. Comput Struct 2018;210:58 – 68.

[23] Chen, X., Kareem, A.. Proper orthogonal decomposition-based modeling, analysis, and simulation of dynamic wind load effects on structures. J Eng Mech 2005;131(4):325–339.

[24] Baker, J.W., Cornell, C.A.. Uncertainty propagation in probabilistic seismic loss estimation. Struct Saf 2008;30(3):236–252.

[25] Suksuwan, A., Spence, S.M.J.. Efficient approach to system-level reliability-based design optimization of large-scale uncertain and dynamic wind-excited systems. ASCE-ASME J Risk Uncertainty Eng Syst, Part A: Civ Eng 2018;4(2).

[26] ASCE 7-16, . Minimum design loads for buildings and other structures. American Society of Civil Engineers (ASCE), Reston, VA; 2017. doi:10.1061/9780784414248. URL https://ascelibrary.org/doi/abs/10.1061/9780784414248.

[27] National Institute of Standards and Technology (NIST), . Extreme wind speed data sets: Hurricane wind speeds. 2016. URL https://www.itl.nist.gov/div898/winds/hurricane.htm.

[28] Li, Y., Kareem, A.. Simulation of multivariate random processes: Hybrid dft and digital filtering approach. J Eng Mech 1993;119(5):1078–1098.

[29] Deodatis, G.. Simulation of ergodic multivariate stochastic processes. J Eng Mech 1996;122(8):778–787.

[30] Chan, C.M., Grierson, D.E., Sherbourne, A.N.. Automatic optimal design of tall steel building frameworks. J Struct Eng 1995;121(5):838–847.

[31] MATLAB, . version 9.3.0.713579 (R2017b). Natick, Massachusetts: The MathWorks Inc.; 2017.

[32] Tokyo Polytechnic University (TPU), . TPU Wind Pressure Database. 2008. URL http://wind.arch.t-kougei.ac.jp/system/eng/contents/code/tpu.

[33] American Society of Civil Engineers (ASCE), . Prestandard for Performance-Based Wind Design. 2019. doi:10.1061/9780784482186. URL https://ascelibrary.org/doi/abs/10.1061/9780784482186.

[34] Minciarelli, F., Gioffrè, M., Grigoriu, M., Simiu, E.. Estimates of extreme wind effects and wind load factors: Influence of knowledge uncertainties. Prob Engng Mech 2001;16:331–340.

[35] Bashor, R., Kijewski-Correa, T., Kareem, A.. On the wind-induced response of tall buildings: the effect of uncertainties in dynamic properties and human comfort thresholds. In: Proc., 10th Americas Conf. on Wind Engineering. 2005,CD-ROM.

[36] Diniz, S.M.C., Sadek, F., Simiu, E.. Wind speed estimation uncertainties: effects of climatological and micrometeorological parameters. Prob Engng Mech 2004;19:361–371.

[37] Spence, S.M.J., Gioffrè, M.. Large scale reliability-based design optimization of wind excited tall buildings. Prob Engng Mech 2012;28:206–215.